THE ASTROPHYSICAL JOURNAL SUPPLEMENT SERIES, 119:141–158, 1998 December

THE INFRARED SPECTRAL CLASSIFICATION OF OXYGEN-RICH DUST SHELLS

G. C. SLOAN[1] AND S. D. PRICE[2]
Received 1997 December 9; accepted 1998 July 13

ABSTRACT

This paper presents infrared spectral classifications for a flux-limited sample of 635 optically identified oxygen-rich variables including supergiants and sources on the asymptotic giant branch (AGB). Several classes of spectra from oxygen-rich dust exist, and these can be arranged in a smoothly varying sequence of spectral shapes known as the *silicate dust sequence*. Classification based on this sequence reveals several dependencies of the dust emission on the properties of the central star. Nearly all S stars show broad emission features from alumina dust, while most of the supergiants exhibit classic features from amorphous silicate dust. Mira variables with symmetric light curves generally show broad alumina emission, while those with more asymmetric light curves show classic silicate emission. These differences may arise from differences in the photospheric C/O ratio.

Subject headings: circumstellar matter — infrared: stars — stars: AGB and post-AGB — stars: fundamental parameters — stars: mass loss

1. INTRODUCTION

Since the launch of the *Infrared Astronomical Satellite* (*IRAS*) in 1982, several authors have developed systems to classify the many types of spectra obtained by the Low-Resolution Spectrometer (LRS). The LRS characterizations introduced in the LRS Atlas (*IRAS* Science Team 1986) and the AutoClass system (Cheeseman et al. 1987; Goebel et al. 1989) classified the entire database of 5425 spectra. In a series of papers, Little-Marenin and collaborators concentrated on the oxygen-rich circumstellar dust shells (Little-Marenin & Price 1986; Little-Marenin & Little 1988, 1990; hereafter referred to as LML classification). They departed from previous methods by not classifying the entire spectrum; instead they concentrated only on the dust emission, which they isolated by estimating and removing the stellar contribution. Their investigation uncovered several distinct and previously unrecognized classes of oxygen-rich dust.

In the LML system, Silicate class emission (Sil) includes spectra with a relatively narrow, classic silicate feature at 10 μm. When this feature is accompanied by an additional component at 11 μm the spectrum becomes Sil+ or Sil++, depending on its strength. Some Sil++ spectra also have an emission feature at 13 μm, which defines the three-component (3c) class in the LML system. The S class in the LML system includes spectra in which the dust emission peaks not at 9.7 μm but rather at $\sim$10.5–10.8 μm. Spectra with a broad, low-contrast emission component peaking at longer wavelengths ($\sim$12 μm) are classified as broad.

Sloan & Price (1995; hereafter Paper I) followed up on the LML system by modifying and quantifying the classification method and applying it to a large sample of sources associated with the asymptotic giant branch (AGB). By using ratios of the spectral emission from the dust shell at 10, 11, and 12 μm, they could organize the entire sample of oxygen-rich dust spectra into a *silicate dust sequence*, which formed the basis for an improved version of the LML classification system.

[1] NASA Ames Research Center, MS 245-6, Moffett Field, CA 94035-1000; sloan@ssa1.arc.nasa.gov.
[2] Phillips Laboratory, PL/GPOB, 29 Randolph Road, Hanscom AFB, MA 01731-3010; price@plh.af.mil.

This paper presents the individual classifications discussed in Paper I and expands the earlier sample to include supergiants and S stars. Section 3 compares the various samples, and § 4 discusses the possible origins of the silicate dust sequence.

2. METHOD

2.1. *The New Samples*

We produced a flux-limited sample of AGB sources by cross-referencing the General Catalogue of Variable Stars (Kholopov et al. 1985–1988; GCVS) with the *IRAS* Point Source Catalog (1988; PSC). We limited the initial sample to variability classes associated with the AGB: Mira, SRa, SRb, and Lb (Hoffmeister, Richter, & Wenzel 1984) and retained only those sources brighter than 28 Jy in the 12 μm filter ([12] < 0.0).

Paper I concentrated on sources with optical spectral types of M or K in order to focus on spectra from oxygen-rich dust, but the AGB sample also included carbon stars, S stars, and sources with unknown optical spectral types (Table 1). The carbon stars are the subject of a separate study (Little-Marenin, Sloan, & Price 1997; Sloan, Little-Marenin, & Price 1998). This paper adds S stars and variability classes associated with supergiants to the sample, since both groups predominately show oxygen-rich dust emission.

The sample of S stars includes more than just the 18 AGB stars identified by optical spectral class in Paper I. Three S stars in the AGB sample were originally included among the carbon stars, but Little-Marenin et al. (1997) found that they possess oxygen-rich dust shells. We have transferred them to the S star sample because the SIMBAD database lists two as S stars and one even as a K5. Three S stars which the GCVS classified as "SR" variables are also included; they are probably SRb variables. Paper I treated weak S stars, i.e., those stars with a strength index of 1 or 2, as MS stars and included them with the oxygen-rich sample. This practice continues here; all MS stars are a part of either the oxygen-rich AGB or supergiant samples.

To compare the properties of dust shells around AGB stars with dust around supergiants, we cross-reference all

TABLE 1

THE SAMPLES

OPTICAL SPECTRAL CLASS	AGB SAMPLE					OTHER SAMPLES			TOTAL
	Mira	SRa	SRb	Lb	Total	SR	SRc	Lc	
M or K......	241	29	157	119	546	...	38	27	611
S	13	2	4	2	21	3	...	...	24
C	31	8	33	24	96	...	...	...	96
None	17	1	...	2	20	...	...	...	20
Total	302	40	194	147	683	3	38	27	751

known SRc and Lc variables from the GCVS with the PSC, uncovering 38 SRc variables and 27 Lc variables brighter than $[12] = 0.0$. All had optical spectral types indicating oxygen-rich photospheres.

2.2. *Classification*

The spectrum for each source in our sample comes from the database from the *IRAS* Low-Resolution Spectrometer maintained at the University of Calgary, which includes the sources published in the LRS Atlas and by Volk & Cohen (1989; hereafter VC). We correct each spectrum as described by Cohen, Walker, & Witteborn (1992).

To isolate the dust spectrum, we assume that the shell is optically thin, so that the total spectrum is a simple sum of contributions from the photosphere and dust shell:

$$S_{\rm LRS}(\lambda) = S_*(\lambda) + S_{\rm dust}(\lambda) . \quad (1)$$

Estimating and removing the stellar contribution isolates the dust contribution. In general,

$$S_*(\lambda) = B(\lambda, T_*)Q_*(\lambda)e^{-\tau_d(\lambda)} . \quad (2)$$

We assume that (1) the low optical depth (τ_d) of the shell allows us to ignore the $e^{-\tau_d}$ term, and (2) the optical efficiencies in the stellar photosphere (Q_*) depend only on the opacity of the H^- ion and on the SiO molecule, so that

$$S_*(\lambda) = E(\lambda, T_*)[1 - Q_{\rm SiO}(\lambda)] , \quad (3)$$

where $E(\lambda, T_*)$ is the Engelke function (Engelke 1992) and $Q_{\rm SiO}$ is the absorption efficiency of photospheric SiO (strongest at 8 μm). An M6 III spectrum characterizes the photosphere of the average AGB source. This corresponds to a 3240 K Engelke function with 15% SiO absorption at 8 μm. We fit our estimated photospheric spectrum to the short-wavelength end of the LRS spectrum and subtract it from all wavelength elements (see Fig. 1). The difference is the contribution from the circumstellar dust shell.

We assign the resulting spectrum to one of several categories by visual inspection (Table 2): naked (N), silicate emission (SE), silicate self-absorption (SB), silicate absorption (SA), or carbon-rich dust emission (CE; usually with a pronounced SiC emission feature at $\sim$11.2 μm). A very small number of sources contain extremely red spectra (H, since they are probably contaminated by emission from H II regions) or are otherwise peculiar, very noisy, or impossible to classify (P). Figure 2 illustrates these spectra, and Table 3 shows the distribution with dust class for each subsample.

These broad categories are analogous to the first digit in the LRS characterizations and the metaclasses in the AutoClass system. VC introduced a system similar to ours (see Table 2). They refer to naked (N) sources as S (for stellar), silicate emission (SE) as E, silicate absorption (SA) as A, and carbon-rich emission (CE) as C. They also define an F class, which contains a mix of lower contrast dust shells. Our classification offers two improvements over

TABLE 2

INFRARED EMISSION CLASSES

Class	Description	VC Class
N	Naked (no dust)	S
SE	Silicate (and oxygen-rich dust) emission	E & F
SB	Silicate self-absorbed emission	E
SA	Silicate absorption	A
CE......	Carbon-rich dust emission	C & F
H	Very red spectrum (possible H II region)	H
P........	Peculiar (or noisy)	

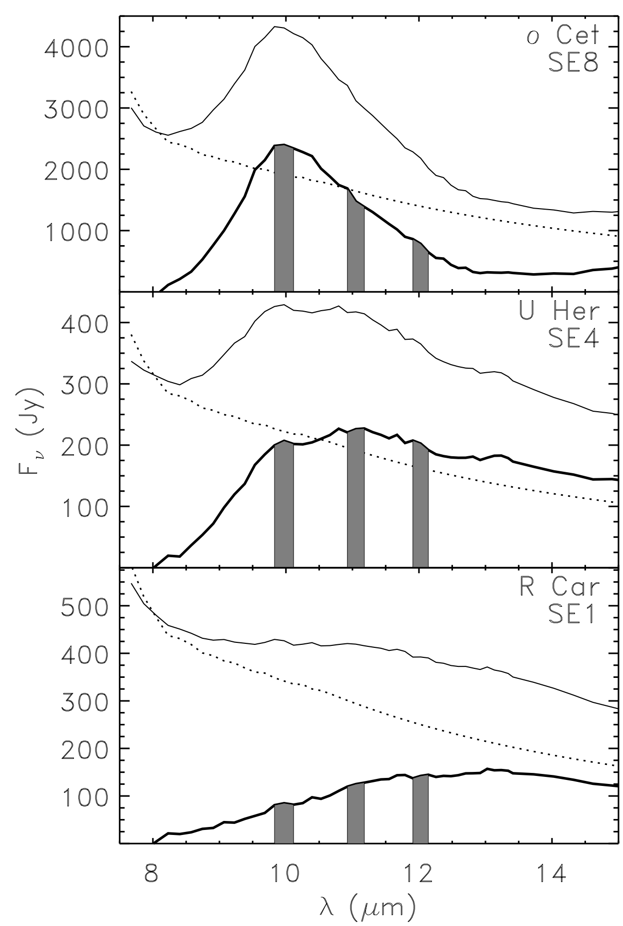

FIG. 1.—Three sample dust extractions. In each of the above panels, we show the corrected LRS spectrum (*thin solid line*), the assumed stellar continuum, (*dotted line*), and the residual dust spectrum (*thick solid line*). The shaded regions show the wavelength ranges over which we determine the flux ratios F_{10}/F_{11} and F_{10}/F_{12}.

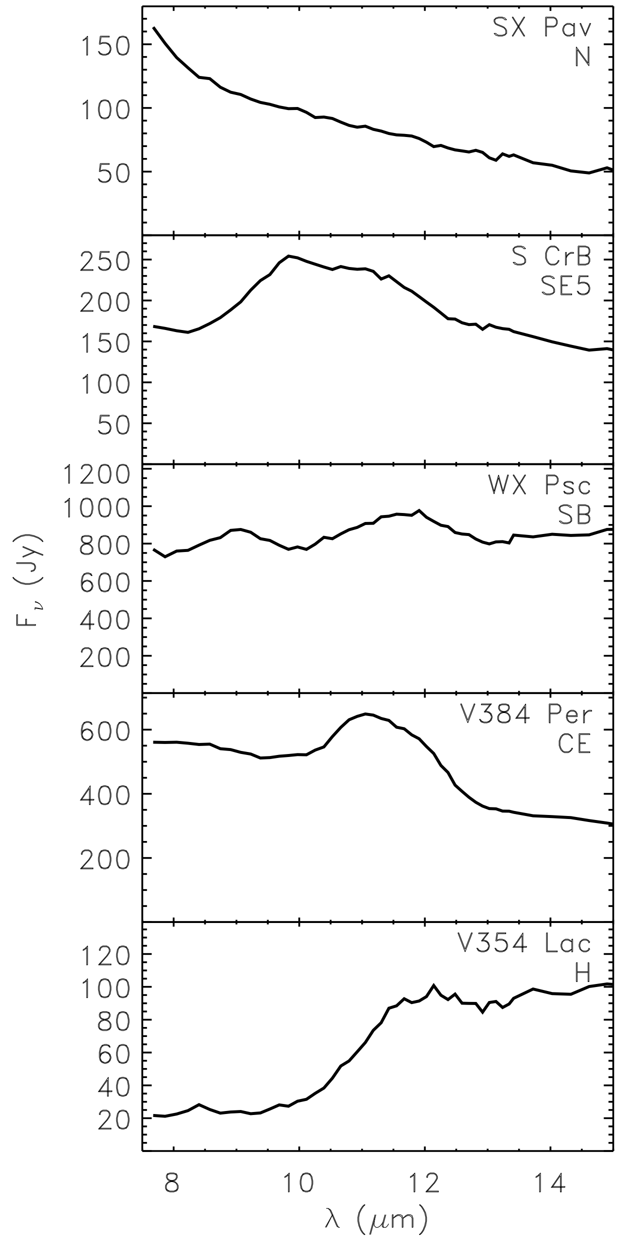

FIG. 2.—Examples of several of the infrared spectral classes observed. Each spectrum is plotted *before* continuum subtraction. The CE spectrum is for a carbon star and is further classified by Sloan et al. (1998) as SiC. We do not include a silicate absorption (SA) spectrum since none appeared in any of our samples or a peculiar (P) spectrum since the three spectra in this class do not resemble each other.

theirs. First, we are able to assign most members of the F class to either SE (generally broad emission, SE1–3) or CE. Second, we recognize self-absorbed silicate emission as a separate class, SB. Kwok, Volk, & Bidelman (1997) present a useful list of classifications as defined by VC for most of the sources observed by the LRS.

2.2.1. *Naked Stars*

The spectrum of naked stars (class N) consists of a stellar photosphere with little or no dust emission (Fig. 2). The border between naked and other classes is not clear-cut, especially for spectra with a low signal-to-noise ratio, where uncertainties in estimating the stellar spectrum can lead to significant uncertainties in the residual dust emission.

TABLE 3

DUST EMISSION CLASSES AMONG THE SUBSAMPLES

Subsample	N	SE	SB	CE	H	P	Total
O-rich AGB:							
Lb	51	67	...	...	1	...	119
SRb	30	126	...	...	...	1	157
SRa	1	28	...	...	...	...	29
Mira	2	232	3	2	...	2	241
Subtotal......	84	453	3	2	1	3	546
Supergiants:							
Lc	9	17	...	...	1	...	27
SRc	4	33	...	...	1	...	38
Subtotal......	13	50	...	...	2	...	65
S stars:							
S.................	4	17	...	3	...	...	24
MS[a]	4	15	...	...	...	...	19
Subtotal......	8	32	...	3	...	...	43

[a] Included in the O-rich AGB and supergiant totals.

The most useful diagnostic is the dust emission contrast, the ratio of the summed emission from the dust to the summed emission from the star over the interval 7.67–14.03 μm. All of our sources with a dust emission contrast less than 4% are classified as naked sources, and all with a dust emission contrast greater than 8% are classified as non-naked. In the transition region between 4% and 8%, we classified sources with lower signal-to-noise ratio as naked, since any dust emission that might exist was impossible to characterize (or even recognize with any confidence).

2.2.2. *Silicate Emission (SE) Sources*

Sources classified as SE show silicate emission (or more precisely, emission from oxygen-rich dust). Plotting the flux ratios F_{10}/F_{12} versus F_{10}/F_{11} places all SE sources on one smooth curve, the *silicate* or *oxygen-rich dust sequence*, which can be parameterized by the power law

$$F_{10}/F_{12} = 1.32(F_{10}/F_{11})^{1.77} . \quad (4)$$

The flux ratios for a given source will not fall exactly on this power law but will fall nearby (Fig. 3). Paper I defined the *corrected flux ratio* F_{11}/F_{12} from the point on the power law closest to the point defined by the actual flux ratios for the source. The corrected flux ratio is the basis for the SE index:

$$\mathrm{SE} = 10(F_{11}/F_{12}) - 7.5 , \quad (5)$$

(truncated, not rounded). Sources that fall outside the SE1–8 range are classified as either SE1 or SE8. Figure 4 presents the sums of all good spectra for each SE index.

Roughly speaking, SE1 and SE2 correspond to the Broad LML class, SE3–4 to Sil++ (and 3c and S), SE5–6 to Sil+, and SE7–8 to Sil. In the discussion below, it is convenient to group these classes in three larger categories: *broad* oxygen-rich dust emission (SE1–2), *structured* silicate emission (SE3–6), and *classic* narrow silicate emission (SE7–8).

2.2.3. *Other Dust Classes*

As the mass-loss rate of an evolved star increases, its shell will grow optically thick. For oxygen-rich dust shells, the silicate emission feature will become self-absorbed (first broadened, then with a noticeable dip at 10 μm) and finally develop into a strong silicate absorption feature. We refer to self-absorbed oxygen-rich dust spectra as SB and fully absorbed spectra as SA. In this nomenclature, a shell will evolve from SE to SB to SA as the mass-loss rate from the

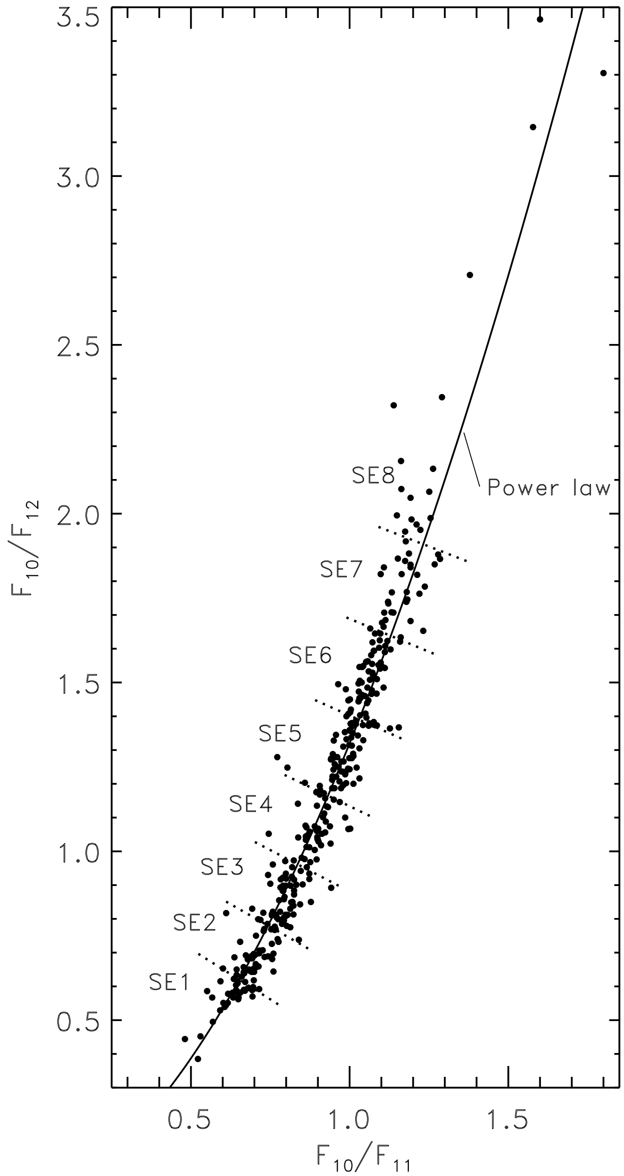

FIG. 3.—The silicate dust sequence, as defined by the flux ratios for individual spectra in the AGB sample (*filled circles*) and a fitted power law (*solid line*).

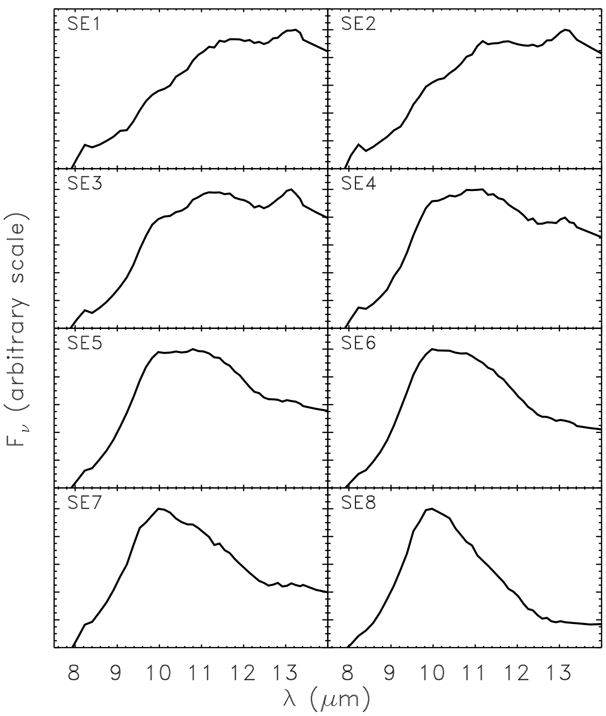

FIG. 4.—Mean spectrum for each of the eight silicate emission (SE) indices, obtained by summing all members in the AGB sample of each index, after removing the stellar spectrum.

central star increases. While SB spectra are rarely identified as such in the literature, SA spectra are commonly seen in OH/IR stars and other sources associated with LRS characterizations between 30 and 39. Our sample of optically identified variables selects against heavily obscured sources, so it is not surprising that no SA spectra appear in our sample. However, the sample does include three SB sources, all long-period Mira variables with very red [12] − [25] colors.

A small number of sources in our sample of oxygen-rich stars show emission from carbon-rich dust emission (CE), usually from silicon carbide dust (Little-Marenin et al. 1997; Sloan et al. 1998). Figure 2 shows that the resemblance between CE spectra and SB spectra is only superficial.

2.2.4. *The 13 μm Feature*

Little-Marenin & Little (1988) first noticed that many of the spectra from oxygen-rich dust contained an emission feature at 13 μm, which they used to define the three-component class. The 13 μm feature appears with all other classes of spectra from oxygen-rich dust, and so we do not consider it when determining the SE index (Paper I). Sources with a 13 μm emission feature are noted by appending a "t" to the SE classification. In a couple of instances, the 13 μm feature is the only dust emission present, which results in a classification of "Nt." The 13 μm sources are treated in more detail by Sloan, LeVan, & Little-Marenin (1996).

2.3. *The Tables*

Tables 4, 5, and 6 present the classifications for the AGB, supergiant, and S star samples. The names of the sources from the PSC are in column (1), followed by the names of the associated sources in the GCVS (col. [2]), the variability class (col. [3]), and the period in days (where known; col. [4]). The spectral type (col. [5]) is generally from the GCVS, but in some cases we replace it with the spectral type from the SIMBAD database or from Bidelman (1980). We use the 12 μm magnitudes ([12]; col. [6]) and [12] − [25] colors (col. [7]) as defined in the PSC. The LRS characterizations (col. [8]) are described in the LRS Atlas. The dust emission contrasts (D.E.C.; col. [9]) are defined in § 2.2.1., and the corrected flux ratios F_{11}/F_{12} (col. [10]) are defined in § 2.2.2. These latter two quantities determine the dust classifications (col. [11]).

3. COMPARING THE SAMPLES

Paper I searched for differences in the types of oxygen-rich dust spectra observed among the four variability classes associated with the AGB (Mira, SRa, SRb, and Lb), but all four classes showed similar distributions of broad, structured, and classic silicate emission. This section recon-

TABLE 4

INFRARED SPECTRAL CLASSIFICATIONS OF THE AGB SAMPLE

PSC (1)	Name (2)	Variability (3)	Period (d) (4)	Spectral Type (5)	[12] (6)	[12] − [25] (7)	LRS (8)	D.E.C. (9)	F_{11}/F_{12} (10)	Dust (11)
00007+5524......	Y Cas	M	413.48	M6–8.5e	−1.34	0.76	22	0.58	1.07	SE3
00042+4248......	KU And	M	750.00	M10 I–III:	−3.06	1.14	26	0.83	1.27	SE5
00050−2546......	SY Scl	M	411.00	M6e–8:	−0.36	0.85	26	0.81	1.35	SE5:
00119−0803......	AD Cet	Lb:	...	M3 III	−0.13	−0.04	18	−0.06	1.14	N:
00121−1912......	AE Cet	Lb:	...	M1 III–3 III	−0.45	−0.07	19	−0.08	1.34	N:
00128−3219......	S Scl	M	362.57	M3–9e(Tc)	−1.41	0.47	15	0.24	1.07	SE3
00205+5530......	T Cas	M	444.83	M6–9.0e	−2.95	0.61	15	0.34	0.93	SE1
00245−0652......	UY Cet	SRb	440.00	M7	−1.53	0.83	14	0.42	1.10	SE3t
00254−1156......	AG Cet	SRb	...	M3	−0.89	0.09	17	0.00	0.00	N
00254−3317......	η Scl	Lb	...	M4 IIIa	−0.51	0.13	18	−0.05	1.53	N:
00340+6251......	TY Cas	M	645.00	M6	−0.63	0.52	28	0.87	1.55	SE7
00445+3224......	RW And	M	430.30	M5–10e(S6,2e)	−0.26	0.83	22	0.38	1.14	SE3:
00484+6238......	VY Cas	SRb	100.00	M6–7	−0.28	0.92	22	0.35	1.13	SE3:
00498+4708......	RV Cas	M	331.68	M4.5–9.5e	−0.13	0.76	23	0.57	1.11	SE3:
00515−6308......	BQ Tuc	Lb:	...	M4 III	−0.42	0.12	...	0.08	1.42	N:
00541+4825......	KS Cas	SRa	454.00	M5	−0.08	0.66	16	0.17	1.14	SE3:t
01030−3157......	AD Scl	M:	...	M9	−0.48	0.50	15	0.25	1.01	SE2:
01037+1219......	WX Psc	M	660.00	M8	−4.03	1.37	...	0.49	0.81	SB
01149+0840......	S Psc	M	404.62	M5–7e	−0.06	0.66	23	0.53	1.21	SE4:
01150+5732......	V465 Cas	SRb	...	M5	−1.02	0.67	41	0.17	1.06	SE3
01217+6049......	BT Cas	M	399.00	M8	−0.67	1.00	23	0.50	1.13	SE3:
01251+1626......	ST Psc	SRb	540.00	M5	−0.19	0.91	28	0.84	1.62	SE8
01261−4334......	γ Phe	Lb:	...	M0 IIIa	−0.98	0.01	16	0.14	0.88	SE1:
01438+1850......	SV Psc	SRb	102.00	M5	−1.08	0.85	23	0.44	1.29	SE5t
01472+5329......	TT Per	SRb	...	M5 II–III	−0.44	0.76	26	0.44	1.53	SE7:
01562+5434......	U Per	M	320.26	M5–7e	−0.66	0.45	15	0.21	0.89	SE1
02036−1027......	UZ Cet	SRa	121.74	M2	−0.46	0.80	...	0.42	1.25	SE4:
02039−5722......	Y Eri	M	302.70	M7e	−0.03	0.53	15	0.16	0.79	SE1:
02143+4404......	W And	M	395.93	S6, 1–9, 2e/M4–M1	−1.93	0.65	22	0.27	1.30	SE5
02145+7831......	AG Cep	M	445.00	M9.2–10e	−0.20	0.68	26	0.82	1.28	SE5
02168−0312......	o Cet	M	331.96	M5–9e	−5.59	0.72	...	0.46	1.92	SE8
02234−0024......	R Cet	M	166.24	M4e–9	−0.03	1.22	29	1.08	1.56	SE8
02251+5102......	RR Per	M	389.62	M6–7e	−0.76	0.60	15	0.32	0.96	SE2
02302+4525......	UX And	SRb	400.00	M6 III	−1.69	1.01	24	0.69	1.31	SE5
02339+3402......	R Tri	M	266.90	M4 III–8e	−0.80	0.40	16	0.12	1.08	SE3
02347+5649......	YZ Per	SRb	378.00	M1 Iab–3Iab	−0.34	1.13	27	0.97	1.42	SE6
02380+3059......	Y Ari	SRb	109.00	M5e	0.00	0.34	17	0.05	0.73	SE1:
02427−5430......	W Hor	SRb	137.00	Mc	−2.01	0.91	22	0.83	1.10	SE3t
02427+6247......	CQ Cas	SRb	300.00	M6.5	−0.47	0.89	...	0.32	1.19	SE4:
02455−1240......	Z Eri	SRb	...	M4 III	−0.87	0.64	25	0.29	1.79	SE8
02455+1718......	T Ari	SRa	316.60	M6–8e	−1.33	0.55	16	0.18	0.94	SE1
02464−5915......	X Hor	SRa	279.60	M6–8e	−0.79	0.55	16	0.15	0.80	SE1t
02497−0828......	RR Eri	SRb	...	M5III	−0.48	0.72	21	0.09	1.30	SE5:
02522−5005......	R Hor	M	407.60	M5–8eII–III	−3.53	0.64	24	0.55	1.33	SE5t
02529+1807......	RZ Ari	SRb	...	M6 III	−1.79	0.08	18	−0.00	5.32	N
02532+5426......	ER Per	SRb	150.00	M6.5	−0.96	0.72	16	0.17	1.34	SE5:t
02568+4356......	AE Per	SRb	115.00	M5	−0.09	0.95	15	0.36	1.08	SE3:
02587+2136......	UZ Ari	Lb:	...	M8	−0.17	0.69	14	0.30	0.83	SE1:t
02596+0353......	α Cet	Lb:	...	M2 III	−2.30	0.00	18	−0.01	1.61	N
03019+3838......	ρ Per	SRb	...	M4 IIb–IIIa	−2.59	0.08	18	−0.01	1.01	N
03082+1436......	U Ari	M	371.13	M4–9.5e	−0.99	0.49	21	0.20	1.19	SE4
03118+4623......	AA Per	SRa	130.40	M7	−0.27	0.90	...	0.44	1.00	SE2:
03170+3150......	UZ Per	SRb	927.00	M5 II–III	−0.89	1.07	25	0.76	1.33	SE5
03172−2156......	τ Eri	Lb	...	M3 III	−1.90	−0.02	17	0.02	0.58	Nt
03318−1619......	RT Eri	M	370.80	M7e	−1.87	0.54	15	0.33	1.05	SE3
03336−7636......	X Men	M	380.00	M3e	−0.58	0.75	26	0.79	1.36	SE6
03415+8010......	SS Cep	SRb	...	M5 III	−1.51	0.77	17	0.08	1.07	SE3
03437−1215......	π Eri	Lb:	...	M2 III	−0.24	0.06	18	−0.03	0.48	N:
03463−0710......	BR Eri	SRb	175.50	M5	−0.24	0.50	17	0.08	0.96	SE2:
03489−0131......	SU Eri	SRb	112.00	M4 III	−1.13	0.74	24	0.52	1.35	SE6
03505−0919......	SW Eri	M	400.69	M9	−0.38	0.62	26	0.76	1.45	SE6t
03507+1115......	IK Tau	M	470.00	M6–10e	−5.54	0.84	26	0.58	1.54	SE7
03511−4558......	U Hor	M	348.40	M6 IIIe	−0.76	0.72	25	0.69	1.30	SE5
03557−1339......	γ Eri	Lb:	...	M0 III	−1.47	0.04	18	−0.02	0.73	N
04094−2515......	W Eri	M	376.63	M7e–9	−1.34	0.66	24	0.56	1.35	SE6
04106+2617......	V482 Tau	Lb:	...	M0–6	−0.11	1.07	...	1.05	1.29	SE5
04140−8158......	U Men	SRa	407.28	Me	−2.70	0.75	24	0.72	1.28	SE5
04157−1837......	RS Eri	M	296.00	M7e	−0.44	0.59	...	0.27	0.98	SE2:
04166+4056......	IR Per	SRa	175.00	M6.5	−2.10	0.96	23	0.59	1.22	SE4t
04250+1555......	W Tau	SRb	264.60	M4–6.5	−0.06	0.72	17	0.06	1.19	SE4:
04255+1003......	R Tau	M	320.90	M5–9e	−1.25	0.84	21	0.38	1.07	SE3

TABLE 4—*Continued*

PSC (1)	Name (2)	Variability (3)	Period (d) (4)	Spectral Type (5)	[12] (6)	[12] − [25] (7)	LRS (8)	D.E.C. (9)	F_{11}/F_{12} (10)	Dust (11)
04265+5718......	RV Cam	SRb	101.00	M4 II–III–6	−0.79	0.99	22	0.27	1.40	SE6t
04280+2722......	V729 Tau	SRb	...	M6	−0.43	0.87	14	0.34	0.90	SE1:t
04311−0004......	BD Eri	M	336.00	M9e	−0.36	0.64	14	0.36	1.03	SE2:
04328+2824......	IU Tau	SRa	418.00	M7	−0.71	0.59	15	0.28	0.95	SE1t
04330+1624......	α Tau	Lb:	...	K5 III	−3.48	−0.09	18	−0.01	1.52	N
04330−6307......	R Ret	M	278.46	M4–7.5e	−0.20	0.44	15	0.16	1.03	SE2:t
04345−2740......	UU Eri	SRb	340.00	M7	−0.22	0.70	15	0.20	0.95	SE2:
04355+0814......	RX Tau	M	331.80	M6–7e	−0.99	0.63	15	0.32	0.92	SE1t
04361−6210......	R Dor	SRb	338.00	M8 IIIe	−5.65	0.29	...	0.16	1.47	SE7t
04382−1946......	DM Eri	SRb	...	M4 III	−0.95	0.06	18	−0.04	1.59	N
04387−3819......	R Cae	M	390.95	M6e	−1.87	0.63	23	0.58	1.14	SE3
04497+1410......	o Ori	SRb	...	M3.2 IIIaS	−1.20	0.06	18	−0.03	1.33	N
04560−0608......	UV Eri	M	433.22	M7	−0.37	0.80	28	1.18	1.44	SE6:
04566+5606......	TX Cam	M	557.40	M8–10	−4.41	0.53	27	1.06	1.38	SE6
05027−2158......	T Lep	M	368.13	M6–9e	−1.86	0.85	15	0.28	0.99	SE2
05069−3434......	SZ Col	Lb:	...	M6	−1.36	0.51	16	0.16	0.95	SE1
05071−6327......	WZ Dor	SRb	...	M3 III	−0.34	0.01	18	−0.05	1.39	N:
05073+5248......	NV Aur	M	635.00	M10	−2.26	1.77	24	0.85	1.06	SB
05090−1154......	RX Lep	SRb	...	M6.2 III	−2.49	0.67	22	0.18	1.38	SE6
05096−4834......	S Pic	M	428.00	M6.5–8 III–IIe	−2.11	0.71	25	0.73	1.36	SE6
05098−6422......	U Dor	M	394.40	M8 IIIe	−1.57	1.03	26	0.76	1.37	SE6
05132+5331......	R Aur	M	457.51	M6.5–9.5e	−3.03	0.56	15	0.37	1.00	SE2
05146+4244......	PU Aur	Lb:	...	M4 III	−0.66	0.00	18	−0.00	0.00	N:
05217−3943......	SW Col	Lb:	...	M1 III	−0.13	1.03	26	0.35	2.00	SE8
05220−0611......	EX Ori	Lb	...	M7 IIIe	−0.51	0.85	14	0.32	0.98	SE2t
05231+5004......	AC Aur	M	311.00	M5e	−0.05	0.79	22	0.43	1.14	SE3:
05256+0839......	V440 Ori	Lb	...	M5	−0.04	0.83	...	0.33	0.95	SE1:
05265−0443......	S Ori	M	414.30	M6.5–9.5e	−1.82	0.62	15	0.24	0.98	SE2
05351−0147......	X Ori	M	422.20	M9	−1.32	0.83	24	0.58	1.25	SE4
05354+2458......	GP Tau	SRb	...	M7	−1.42	0.95	22	0.50	1.22	SE4
05365−1404......	RW Lep	SRa	149.90	M8	−0.98	0.68	15	0.23	0.82	SE1t
05367+3736......	RU Aur	M	466.47	M7–9e	−1.84	0.86	25	0.80	1.28	SE5
05368+2841......	AW Aur	M	695.00	M5–9	−0.11	0.75	15	0.36	1.09	SE3:
05378+2804......	AB Tau	SRa	142.00	M5–7	−0.88	0.86	15	0.32	1.11	SE3
05384+3854......	SZ Aur	M	454.04	M8e	−0.84	0.57	15	0.30	1.04	SE2t
05388+3200......	U Aur	M	408.09	M7–9e	−1.53	0.75	23	0.44	1.22	SE4:
05390+1448......	FX Ori	SRb	720.00	M3	−0.22	0.91	25	0.63	1.57	SE8t
05404−2343......	RT Lep	M	399.00	M9e	−1.06	0.81	22	0.47	1.08	SE3
05411−8625......	R Oct	M	405.39	M5.5e	−1.26	0.75	15	0.27	0.92	SE1
05450−3142......	S Col	M	325.85	M6e–8	−0.57	0.67	14	0.38	1.00	SE2
05528+2010......	U Ori	M	368.30	M6–9.5e	−3.46	0.51	26	0.81	1.37	SE6t
05534+4530......	TW Aur	SRb	150.00	M5 III	−1.67	0.75	25	0.83	1.36	SE6t
05535+4822......	LO Aur	M	...	M8–9	−0.40	1.07	28	1.10	1.43	SE6
05559+7430......	V Cam	M	522.45	M7e	−2.14	0.85	24	0.69	1.22	SE4
05588+1054......	DP Ori	SRb	...	M6.5	−0.38	0.67	15	0.27	1.11	SE3t
05592−0221......	V352 Ori	Lb	...	M7ep	−1.85	0.94	...	0.49	1.35	SE6
06011+2829......	BS Aur	M	462.00	M8–9	−0.95	0.83	28	1.04	1.41	SE6
06036−2411......	S Lep	SRb	...	M6 III	−2.40	0.90	26	0.83	1.41	SE6t
06067+3125......	BU Aur	SRa	169.00	M1	−0.61	0.54	...	0.30	1.04	SE2:
06133+6132......	UW Lyn	Lb:	...	M3 IIIab	−0.93	0.02	18	−0.02	1.76	N
06139+3313......	VW Aur	SRb	220.00	M6	−1.44	0.81	22	0.48	1.20	SE4t
06199+2232......	μ Gem	Lb	...	M3.0 IIIab	−2.58	0.01	18	−0.02	1.49	N
06202−0210......	V Mon	M	340.50	M5–8e	−0.99	0.39	16	0.13	0.94	SE1
06224+1701......	GN Ori	M	118.30	M7	−0.78	0.26	44	0.21	0.71	SiC
06250+6134......	V Lyn	SRb	...	M5 III–IV	−0.34	1.20	23	0.47	1.32	SE5:t
06261+1637......	AQ Gem	Lb	...	M6.5–8	−0.44	0.79	15	0.31	0.96	SE2:
06278+2729......	DW Gem	Lb	...	M3–7	−1.89	0.75	27	0.80	1.48	SE7
06300+3137......	AL Aur	M	385.71	M7e	−0.01	0.55	25	0.80	1.30	SE5:
06333−0520......	GL Mon	SRb	103.50	M4–6.5	−1.22	0.51	16	0.16	0.81	SE1
06349−0121......	SY Mon	M	422.17	M6e–9	−1.80	0.76	25	0.77	1.32	SE5
06363+5954......	U Lyn	M	433.60	M7–9.5:e	−1.48	0.63	27	0.98	1.40	SE6
06423+0905......	FX Mon	M	428.50	M1–8	−0.67	0.72	28	1.06	1.40	SE6
06431+1543......	UX Gem	M	466.00	M8	−0.28	0.56	27	0.84	1.30	SE5:
06434−3628......	CH Pup	M	505.50	Me	−0.57	0.83	23	0.52	1.19	SE4
06439+3019......	X Gem	M	264.16	M5–8e(Tc:)	−0.08	0.53	17	0.13	1.11	SE3:
06496−1858......	DL CMa	M	345.00	M7e	−1.01	0.99	26	0.75	1.36	SE6
06500+0829......	GX Mon	M	527.00	M9	−3.32	1.00	28	0.91	1.45	SE6
06534−1647......	GS CMa	Lb:	...	M7	−0.11	1.04	22	0.50	1.25	SE5:t
06546−2353......	X CMa	SRb	106.60	M7	−0.96	0.87	23	0.54	1.26	SE5t
06551+0322......	AZ Mon	M	388.90	M9	−0.28	0.64	22	0.56	1.14	SE3:t
07021−0852......	HN Mon	M	410.00	M8	−1.59	0.97	29	1.37	1.44	SE6

TABLE 4—*Continued*

PSC (1)	Name (2)	Variability (3)	Period (d) (4)	Spectral Type (5)	[12] (6)	[12] − [25] (7)	LRS (8)	D.E.C. (9)	F_{11}/F_{12} (10)	Dust (11)
07091−2902......	GW CMa	Lb	...	M5	−0.51	0.73	14	0.34	0.90	SE1:t
07104+1614......	BQ Gem	SRb	...	M4 IIIab	−0.87	0.10	17	0.02	0.77	N
07120−4433......	L Pup	SRb	140.60	M5 III–6IIIe	−4.83	0.42	...	0.60	0.00	:(P)
07229+3328......	XX Gem	M	384.05	M9–10e	−0.22	0.64	22	0.45	1.09	SE3:
07232−0544......	TT Mon	M	323.17	M5e–8	−0.48	0.78	23	0.46	1.37	SE6:
07299+0825......	S CMi	M	332.94	M6–8e	−1.40	0.56	15	0.25	0.96	SE2
07304−2032......	Z Pup	M	508.60	M4–9e	−1.60	0.81	29	1.34	1.39	SE6
07329−2352......	DU Pup	M	550.00	M	−1.69	1.13	27	0.99	1.34	SE5
07382+2032......	Y Gem	SRb	160.00	M6e–7	−0.01	0.31	17	0.08	1.20	SE4:
07445−2613......	SS Pup	M	391.00	M6e	−1.10	0.75	29	1.31	1.44	SE6
07518−2612......	OR Pup	Lb:	...	M7	−0.53	0.14	18	−0.02	0.90	N:
07536−2830......	HU Pup	SRa	238.00	M3	−1.20	1.52	28	1.46	1.31	SE5
07543−3008......	PX Pup	Lb:	...	M6 III	−0.40	0.17	17	0.01	1.18	N:
07585−1242......	U Pup	M	318.44	M5–8e	−1.27	0.97	25	0.80	1.31	SE5
08003+3629......	SV Lyn	SRb	...	M5 III	−0.66	0.94	23	0.21	1.44	SE6:
08063+6522......	RZ UMa	SRb	115.00	M5–6	−0.54	0.75	16	0.18	1.07	SE3:
08078−3801......	AS Pup	M	324.65	M7e–9	−1.48	0.55	15	0.29	0.93	SE1
08084−1510......	DP Pup	M	...	M8e	−0.28	0.99	29	1.19	1.37	SE6:
08107−3459......	Y Pup	SRb	110.00	M7	−0.36	0.49	22	0.15	1.38	SE6
08117+2453......	RX Cnc	SRb	120.00	M8	−0.22	0.38	16	0.07	0.69	SE1:
08138+1152......	R Cnc	M	361.60	M6–9e	−2.54	0.49	15	0.24	1.01	SE2
08150−3117......	NN Pup	M	...	M7e	−0.23	0.65	21	0.35	0.97	SE2:
08189+0507......	FZ Hya	Lb	...	M6	−1.07	0.81	21	0.33	1.16	SE4t
08196+1509......	Z Cnc	SRb	104.00	M6 III	−0.48	0.80	24	0.49	1.37	SE6:t
08200−2528......	OT Pup	Lb	...	M4	−0.50	1.10	24	0.78	1.23	SE4:
08220−0821......	FK Hya	Lb	...	Mb	−2.20	0.89	29	1.31	1.51	SE7t
08239+1249......	BP Cnc	SRb	...	M3 III	−0.03	0.02	18	−0.00	0.00	N:
08272−0609......	RT Hya	SRb	290.00	M6–8e	−1.44	0.53	16	0.11	0.57	SE1
08349−5945......	KK Car	M	...	M5ep	−1.59	0.57	21	0.40	1.06	SE3
08375−1707......	AK Hya	SRb	...	M4 III	−2.08	0.77	22	0.32	1.25	SE4t
08400−4755......	EP Vel	SRa	240.00	M6	−1.13	1.01	26	1.01	1.30	SE5
08437+0149......	EY Hya	SRa	182.70	M7	−1.39	0.79	...	0.44	0.95	SE2
08555+1102......	RT Cnc	SRb	...	M5 III	−1.03	0.56	41	0.25	1.12	SE3
09005+3856......	UX Lyn	SRb:	...	M6 III	−0.24	0.13	17	0.01	0.00	N:
09057+1325......	CW Cnc	Lb	...	M6	−1.25	0.82	15	0.34	1.07	SE3
09069+2527......	W Cnc	M	393.22	M6.5–9e	−0.89	0.83	23	0.43	1.16	SE4
09105−4334......	SY Vel	SRb	...	M5/6 III	−0.96	0.84	24	0.40	1.51	SE7
09175−5010......	DM Vel	SRb:	175.00	M6	−0.13	0.68	15	0.20	1.00	SE2:t
09180+5654......	CG UMa	Lb	...	M4 IIIa	−0.38	0.15	18	−0.03	0.00	N:
09185−4918......	RW Vel	M	443.10	M7 III(II)e	−2.34	0.59	15	0.29	0.96	SE2
09220−4839......	RS Vel	M	409.50	M7e	−2.11	0.69	21	0.39	1.04	SE2
09273−5157......	Y Vel	M	449.90	M8e–9.5	−1.15	0.78	23	0.47	1.20	SE4
09309−6234......	R Car	M	308.71	M4–8e	−3.06	0.45	15	0.21	0.95	SE1
09331−1428......	X Hya	M	301.10	M7–8.5e	−1.34	0.55	15	0.34	1.00	SE2
09425+3444......	R LMi	M	372.19	M6.5–9.0e(Tc:)	−2.94	0.60	24	0.74	1.20	SE4t
09429−2148......	IW Hya	M:	650.00	M9	−3.32	1.34	28	1.18	1.27	SE5
09429+5721......	CS UMa	Lb:	...	M3 IIIab	−0.38	0.08	17	0.02	0.00	N:
09448+1139......	R Leo	M	309.95	M6–8 III–9.5e	−4.71	0.26	...	0.23	0.99	SE2
09480−4147......	SU Vel	SRb	150.00	M5(III)	−1.80	1.00	15	0.34	1.05	SE3t
09481−4425......	SZ Vel	SRb	150.00	M5e	−0.48	0.83	22	0.34	1.25	SE5:
09511−5356......	Z Vel	M	411.40	M9e	−1.16	0.55	15	0.28	0.89	SE1t
09564−5837......	RR Car	SRb	...	M6.5S II–III	−1.89	0.68	15	0.22	0.96	SE2
10118−6038......	SU Car	M	575.60	M5–8e	−0.63	1.02	29	1.51	1.47	SE7
10133−5413......	W Vel	M	394.72	M5–8 IIIe	−1.57	0.62	22	0.50	1.10	SE3t
10147−5057......	GY Vel	Lb	...	M4/5 III	−0.18	0.12	17	0.00	0.00	N:t
10189−3432......	V Ant	M	302.76	M7 IIIe	−1.02	1.00	28	1.02	1.49	SE7
10226−6039......	UV Car	Lb	...	M3–5	−0.64	1.23	29	2.84	1.40	SE6
10261−5055......	VZ Vel	SRa	317.00	M6e	−0.28	1.02	27	0.75	1.53	SE7
10305+7001......	CT UMa	Lb	...	M6	−0.16	0.71	22	0.26	1.11	SE3
10353−1145......	FF Hya	SRb	...	M6	−0.93	0.97	...	0.33	1.17	SE4:
10401−5327......	HH Vel	SRb	100.00	M5/6 III	−1.03	1.08	26	0.85	1.42	SE6t
10411+6902......	R UMa	M	301.62	M3–9e	−1.30	0.97	23	0.42	1.35	SE6
10469−5355......	WX Vel	M	411.50	M5–7 IIIe	−0.23	0.78	22	0.50	1.11	SE3:
10521+7208......	VX UMa	M	215.20	M8e	−0.25	0.94	26	0.83	1.33	SE5
10580−1803......	R Crt	SRb	160.00	M7	−3.38	0.77	22	0.64	1.10	SE3t
11010−0256......	SX Leo	SRb	100.00	M6	−0.10	0.55	16	0.15	0.94	SE1:
11011−6651......	KV Car	SRb	150.00	M4 III	−0.44	0.77	43	0.25	1.27	SE5:
11065+3634......	CO UMa	Lb	...	M3.5 IIIab	−0.27	0.11	17	−0.01	0.00	N:
11125+7524......	CS Dra	Lb	...	M5	−1.27	0.90	23	0.60	1.25	SE4:t
11153−2152......	RX Crt	SRb	300.00	M3	−0.10	0.20	17	0.03	1.13	N:t
11251+4527......	ST UMa	SRb	110.00	M4–5 III	−0.48	0.64	...	0.16	1.09	SE3:
11252+1525......	AF Leo	SRb	107.00	M5	−0.57	1.08	...	0.65	1.20	SE4:

TABLE 4—*Continued*

PSC (1)	Name (2)	Variability (3)	Period (d) (4)	Spectral Type (5)	[12] (6)	[12] − [25] (7)	LRS (8)	D.E.C. (9)	F_{11}/F_{12} (10)	Dust (11)
11358+0824......	ω Vir	Lb	...	M4 III	−0.86	0.06	18	−0.05	1.29	N
11445+4344......	AZ UMa	Lb	...	M6 III	−1.06	1.19	...	0.42	1.18	SE4
11462−2628......	II Hya	SRb	...	M4 III	−0.93	0.07	18	−0.02	0.79	N
11466−4128......	X Cen	M	315.10	M5–6.5e	−1.56	0.52	23	0.37	1.35	SE6
11485−1055......	RU Crt	Lb:	...	M3	−1.15	0.51	...	0.14	1.06	SE3:
11501−0719......	S Crt	SRb	155.00	M6–7e	−0.69	0.63	16	0.20	1.21	SE4:
11538+5808......	Z UMa	SRb	195.50	M5 IIIe	−0.89	0.57	16	0.11	0.89	SE1t
12020+0254......	TZ Vir	SRb	134.00	M5	−0.08	1.01	26	0.68	1.31	SE5:
12046−0629......	RW Vir	Lb	...	M5 III	−1.21	0.61	...	0.35	1.13	SE3t
12148−6741......	ϵ Mus	SRb:	...	M5 III	−2.08	0.07	18	−0.01	1.28	N
12170−1858......	R Crv	M	317.03	M4.5–9:e	0.00	0.41	...	0.33	0.63	P:
12230−5943......	ST Cru	M	440.00	M6e	−1.70	0.72	23	0.51	1.21	SE4
12277+0441......	BK Vir	SRb	150.00	M7 III	−2.36	0.59	15	0.24	1.15	SE4t
12279+6928......	CQ Dra	Lb:	...	M3 IIIa	−0.31	0.04	18	−0.03	1.24	N
12295−5718......	U Cru	M	342.60	M4–6e	−0.71	0.82	24	0.61	1.35	SE6
12319−6728......	BO Mus	Lb	...	M6 II–III	−1.69	0.20	17	0.02	0.44	N
12345−1715......	T Crv	M	401.34	M6e	−0.22	0.63	...	0.45	1.02	SE2:
12380+5607......	Y UMa	SRb	168.00	M7 II–III:	−2.08	0.75	15	0.27	1.00	SE2t
12517−0915......	ψ Vir	Lb	...	M3 III	−0.55	−0.08	18	−0.03	1.15	N:
12526+4728......	TU CVn	SRb	...	M5 III	−0.77	0.11	...	−0.01	5.40	N:
12562+2324......	T Com	M	406.00	M2:–8–9e III	−0.19	0.98	28	0.87	1.57	SE8
13001+0527......	RT Vir	SRb	155.00	M8 III	−3.03	0.78	21	0.46	1.07	SE3t
13039+2253......	FS Com	SRb	...	M5 III	−0.89	0.10	18	−0.01	0.00	N
13062−5958......	WW Cen	SRb	304.00	M5–7	−0.03	0.48	31	0.10	0.65	SE1:
13114−0232......	SW Vir	SRb	150.00	M7 III	−3.45	0.81	...	0.41	1.12	SE3t
13144−6225......	V397 Cen	Lb:	...	M4(S:)	−1.04	1.08	...	2.45	1.20	SE4t
13150−4124......	V497 Cen	M	335.00	Me	−0.92	0.67	14	0.37	0.95	SE2
13172+4547......	V CVn	SRa	191.89	M4–6e IIIa:	−1.67	0.77	29	1.00	1.69	SE8t
13215−6424......	U Mus	M	356.00	M6e	−0.24	0.57	15	0.28	0.95	SE2:
13244−5904......	OS Cen	M	433.00	M6e	−0.72	0.92	41	0.50	0.99	SE2
13269−2301......	R Hya	M	388.87	M6–9eS(Tc)	−4.37	0.48	15	0.24	0.98	SE2t
13303−0656......	S Vir	M	375.10	M6 III–9.5e	−1.70	0.58	16	0.19	0.97	SE2
13368−4941......	V744 Cen	SRb	...	M8 III	−2.24	0.84	22	0.36	1.21	SE4
13462−2807......	W Hya	SRa	361.00	M7.5–9ep	−5.43	0.19	02	0.10	2.22	SE8
13465−3412......	V806 Cen	SRb	...	M5 III	−2.39	−0.04	18	0.01	1.40	N
13468+3947......	R CVn	M	328.53	M5.5–9e	−1.40	0.55	15	0.24	1.07	SE3
13492−0325......	AY Vir	SRb	113.00	M6	−0.54	0.74	16	0.21	1.15	SE4:
13499+6458......	CU Dra	Lb:	...	M3 III	−0.73	0.12	18	−0.01	1.20	N
13548−3049......	TW Cen	M	269.27	M4e–8II:	−0.54	0.46	22	0.23	1.25	SE5:
13574+3726......	RW CVn	SRb	100.00	M7 III	−0.08	0.81	...	0.28	1.05	SE2:
14003−7633......	θ Aps	SRb	32.04	M7 III	−3.54	0.72	22	0.29	1.27	SE5t
14020−3515......	AQ Cen	M	387.50	Me	−2.32	0.54	29	1.26	1.47	SE7
14059+4405......	BY Boo	Lb:	...	M4–4.5 III	−0.97	0.13	18	−0.03	1.34	N
14081−1604......	ET Vir	SRb	...	M2 IIIa	−0.04	0.08	...	−0.04	1.27	N:
14086−2839......	RU Hya	M	331.50	M6–8.8e	−1.09	0.82	26	0.69	1.52	SE7t
14129−5940......	R Cen	M	546.20	M4–8 IIe	−3.09	0.58	22	0.78	1.05	SE2
14142−1612......	EW Vir	SRb	...	M6 III	−0.88	0.89	22	0.45	1.12	SE3
14162+6701......	U UMi	M	330.92	M6–8e	−0.85	0.58	15	0.20	0.95	SE2
14167−6717......	UZ Cir	M	538.00	Me	−0.02	0.77	22	0.54	1.06	SE3t
14188−6943......	VX Cir	M	417.00	M7e	−0.19	0.56	...	0.49	1.20	SE4:
14200+2935......	CI Boo	Lb	...	M3 III	−0.14	0.20	...	−0.05	1.80	N
14219+2555......	RX Boo	SRb	340.00	M6.5–8 IIIe	−3.69	0.80	...	0.48	1.07	SE3t
14247+0454......	RS Vir	M	353.95	M6 III–8e	−1.46	1.01	24	0.56	1.35	SE5
14277+3904......	V Boo	SRa	258.01	M6e	−0.42	0.41	16	0.16	1.03	SE2:
14280−2952......	Y Cen	SRb:	180.00	M4e–7	−1.84	0.60	16	0.15	0.92	SE1t
14310−6044......	V798 Cen	Lb:	...	M6 III	−0.58	0.43	17	0.09	0.75	SE1:
14371+3245......	RV Boo	SRb	137.00	M5–7e	−1.61	0.93	22	0.39	1.26	SE5t
14390+3147......	RW Boo	SRb	209.00	M5	−0.84	0.78	23	0.28	1.45	SE7
14412+2644......	W Boo	SRb:	450.00	M2–4 III	−0.36	0.08	18	−0.06	1.10	N
14455−3625......	V768 Cen	SRb	...	M3	−1.21	0.16	18	0.01	0.00	N
14550−1214......	FY Lib	SRb	120.00	M5 III	−1.27	0.73	22	0.24	1.28	SE5
14559−5446......	Y Lup	M	396.82	M7e	−1.37	0.87	24	0.64	1.29	SE5
14567+6607......	RR UMi	SRb	...	M5 III	−1.61	0.12	18	−0.01	0.00	N
14580−3416......	AP Cen	M	357.00	M5e	0.00	0.50	15	0.25	1.10	SE3:
14598−7124......	V Aps	Lb	...	Mb	−0.40	0.97	22	0.63	1.15	SE3:t
15011−2505......	σ Lib	SRb	...	M3.5 IIIa	−2.13	−0.11	18	0.00	0.00	N
15014−4040......	GM Lup	Lb:	...	M6 III	−0.41	0.10	18	−0.02	4.28	N:
15097+1909......	FL Ser	Lb	...	M4 IIIab	−0.07	0.05	...	0.03	0.00	N:
15193+1429......	S Ser	M	371.84	M5–6e	−0.45	0.63	22	0.48	1.12	SE3:
15193+3132......	S CrB	M	360.26	M6–8e	−2.13	1.05	24	0.64	1.27	SE5
15214−2244......	RS Lib	M	217.65	M7–8.5e	−2.06	0.41	15	0.30	0.97	SE2
15239−5733......	R Cir	SRb	222.00	M4/6 III	−0.45	0.49	16	0.15	0.74	SE1:

TABLE 4—*Continued*

PSC (1)	Name (2)	Variability (3)	Period (d) (4)	Spectral Type (5)	[12] (6)	[12] − [25] (7)	LRS (8)	D.E.C. (9)	F_{11}/F_{12} (10)	Dust (11)
15255+1944......	WX Ser	M	425.10	M8e	−2.30	1.08	29	1.59	1.38	SE6
15298+0348......	WW Ser	M	365.80	M8e	−0.48	0.65	14	0.34	0.95	SE1t
15303−2700......	SV Lib	M	402.66	M8e	−0.21	0.51	22	0.22	1.14	SE3:
15314+7847......	S UMi	M	331.00	M6–9e	−1.78	0.58	21	0.32	1.08	SE3t
15323−4920......	R Nor	M	507.50	M3e–6 II	−0.75	0.89	23	0.50	1.20	SE4
15341+1515......	τ Ser	SRb	100.00	M5 IIb–IIIa	−2.06	0.77	22	0.22	1.24	SE4
15361+2441......	LY Ser	Lb:	...	M4 III	−1.24	0.17	17	0.03	0.92	N
15380−6545......	IZ TrA	Lb	...	M6 III	−0.80	0.66	16	0.16	0.92	SE1t
15402−5449......	T Nor	M	240.70	M3–6e	−0.77	0.74	25	0.43	1.81	SE8
15410−0133......	BG Ser	M	143.00	M6–8e	−1.56	0.55	21	0.38	1.08	SE3
15483+1517......	R Ser	M	356.41	M5 III–9e	−2.07	0.49	24	0.47	1.33	SE5
15492+4837......	ST Her	SRb	148.00	M6–7 IIIaS	−2.12	0.78	41	0.21	0.90	SE1
15566+3609......	RS CrB	SRa	332.20	M7	−0.67	0.87	26	0.90	1.40	SE6t
15576−1212......	FS Lib	M	415.00	M8.1–9.0	−0.55	1.02	29	1.24	1.41	SE6
16011+4722......	X Her	SRb	...	M6e	−3.08	0.80	24	0.53	1.39	SE6t
16030−2135......	Z Sco	M	343.03	M5.5:–7e	−0.12	0.50	16	0.08	0.00	N:
16061+0844......	FQ Ser	Lb	...	M4 III	−0.17	0.06	...	−0.17	1.32	N
16063−4906......	V Nor	SRb	155.90	M5 III	−0.75	0.36	17	0.06	0.76	SE1:t
16081+2511......	RU Her	M	484.83	M6e–9	−1.96	0.70	23	0.64	1.12	SE3
16095+2337......	LQ Her	Lb:	...	M4 IIIa	−0.51	0.08	17	−0.01	0.00	N:
16118−4439......	RU Nor	M	393.30	M7e	−0.05	0.75	15	0.29	0.93	SiC
16127−7834......	δ Aps	Lb:	...	M4–5 III	−1.34	0.12	18	−0.01	0.00	N
16128−5228......	W Nor	SRb	134.70	M4/5(III)	−0.94	0.69	...	0.52	1.22	SE4:
16164+5952......	AT Dra	Lb	...	M4 IIIa	−0.58	0.15	18	−0.00	0.00	N
16175−6120......	RS TrA	M:	436.40	Me	−0.06	0.56	15	0.28	1.02	SE2:
16235+1900......	U Her	M	406.10	M6.5–9.5e	−3.12	0.45	23	0.55	1.19	SE4
16241−3111......	WW Sco	M	431.00	M6e–9	−0.15	0.59	15	0.26	0.99	SE2:
16250−0729......	V2105 Oph	SRb:	...	M2.5 III	−0.15	0.05	18	−0.02	1.27	N:
16260+3454......	V697 Her	M	475.00	M9	−0.86	1.32	28	1.11	1.40	SE6
16265−1914......	Y Sco	M:	351.88	M8	−0.02	0.60	15	0.33	0.86	SE1:
16269+4159......	ZZ Her	SRb	...	M6 III	−2.97	0.39	16	0.08	0.78	SE1t
16306+7223......	R UMi	SRb	325.70	M7 IIIe	−1.43	0.64	15	0.29	1.01	SE2t
16308−1601......	T Oph	M	366.82	M6.5e	−0.32	0.65	15	0.30	0.88	SE1:
16387−2700......	AX Sco	SRb	138.00	M6	−0.56	0.63	15	0.21	1.12	SE3t
16418+5459......	S Dra	SRb	136.00	M7	−1.66	0.93	24	0.53	1.34	SE5t
16432+1213......	UV Her	M	341.95	M6–6.5e	−0.25	0.48	15	0.18	1.03	SE2:
16457+4219......	V636 Her	Lb	...	M4 III–IIIa	−0.04	0.16	18	−0.02	0.67	N:
16473+5753......	AH Dra	SRb	158.00	M7	−0.87	0.50	22	0.19	1.38	SE6:
16496+1501......	S Her	M	307.28	M4,S–7.5,Se	−0.21	0.37	17	0.06	1.07	N:
16520−4501......	RS Sco	M	319.91	M5e–9	−1.71	0.67	...	0.27	1.11	SE3
16521−2153......	SY Oph	SRb	132.00	M5	−0.99	0.85	42	0.40	1.11	SE3
16534−3030......	RR Sco	M	281.45	M6 II–IIIe–9	−2.06	0.49	15	0.21	1.06	SE3t
17001−3651......	RT Sco	M	449.04	S7,2(M6–M7e)	−1.88	0.61	22	0.37	1.10	SE3
17043−3145......	TU Sco	M	373.04	M7 IIe–9	−0.17	0.87	23	0.39	1.26	SE5:
17048−1601......	R Oph	M	306.50	M4–6e	−0.91	0.43	16	0.15	1.05	SE3:
17079−7405......	W Aps	Lb	...	M6	−0.58	0.93	21	0.44	1.13	SE3t
17081+6422......	TV Dra	Lb	...	M8p(S)	−0.82	0.64	15	0.20	0.92	SE1t
17086+2739......	CX Her	SRb	114.00	M7	−0.04	0.61	15	0.23	1.18	SE4:
17115−3322......	RW Sco	M	388.45	M5e	−1.69	0.95	27	0.82	1.37	SE6
17123+1107......	V438 Oph	SRb	169.90	M0–7e	−0.84	0.65	15	0.18	0.90	SE1t
17123−2122......	V1699 Oph	Lb	...	M8	−0.03	0.77	15	0.23	1.12	SE3:
17139+0446......	UY Oph	M	332.00	M7 III	−0.71	0.57	27	0.99	1.45	SE6:
17141−1737......	V1769 Oph	M	...	M8–10	−0.46	0.74	25	0.81	1.36	SE6
17236+1657......	V640 Her	Lb	...	M4 IIIab	−0.07	0.09	17	0.00	0.00	N:
17296+3231......	KT Her	M	381.00	M6e	−0.04	0.66	28	1.05	1.45	SE6
17334+1537......	MW Her	M	449.00	M8–9	−1.84	1.11	29	1.17	1.43	SE6
17343+1052......	V790 Oph	M	370.00	M5 IIIe	−0.31	0.66	25	0.70	1.47	SE7:t
17361+5746......	TY Dra	Lb	...	M5–8	−0.92	1.16	28	0.94	1.59	SE8t
17387−4343......	RU Sco	M	370.75	M4/6–7 II–IIIe	−0.90	0.44	16	0.17	0.89	SE1
17388−1645......	BG Oph	M	342.50	M9	−0.71	0.95	26	0.70	1.37	SE6
17398−4344......	TV Sco	SRb	200.00	Me	−0.69	0.83	41	0.51	1.05	SE3
17445−4414......	QX Sco	M	360.00	Me	−0.07	0.52	14	0.38	1.05	SE3:
17468−2900......	V758 Sgr	Lb	...	M2	−0.59	0.97	...	1.03	1.36	SE6
17508−3419......	BN Sco	M	616.00	M6	−0.74	0.90	22	0.51	1.17	SE4t
17513−2313......	V774 Sgr	Lb	...	M5	−2.19	1.20	29	2.00	1.41	SE6
17531−4947......	W Ara	SRb	126.00	M5 III	−0.10	0.83	15	0.28	0.95	SE1:t
17538−3728......	V438 Sco	M	392.00	M3e	−0.69	0.87	24	0.54	1.33	SE5
17540−1919......	VV Sgr	M	401.50	M3–8e	−1.18	0.45	28	0.87	1.46	SE7
17541+1110......	RT Oph	M	426.34	M7e(C)	−0.80	0.71	22	0.63	1.09	SE3t
17553+4521......	OP Her	SRb	120.50	M5 IIb–IIIa(S)	−0.70	0.31	17	0.01	0.44	N
17579+2335......	WY Her	M	376.00	M5–7e	−0.86	0.95	29	1.09	1.62	SE8
18004−2259......	V1951 Sgr	M	510.00	M9	−0.30	0.63	23	0.49	1.19	SE4

TABLE 4—*Continued*

PSC (1)	Name (2)	Variability (3)	Period (d) (4)	Spectral Type (5)	[12] (6)	[12] − [25] (7)	LRS (8)	D.E.C. (9)	F_{11}/F_{12} (10)	Dust (11)
18018−2802......	V1804 Sgr	M:	...	M9.5	−1.73	0.96	28	0.97	1.48	SE7
18125−7741......	BR Oct	Lb:	...	M4–6	−0.51	0.85	23	0.49	1.32	SE5
18142−3646......	η Sgr	Lb:	...	M3.5 III	−2.20	−0.00	18	−0.01	1.80	N
18157+1757......	IQ Her	SRb	...	M4	−0.89	0.33	17	0.08	1.35	SE6:
18183+0554......	V1014 Oph	Lb	...	M5e	0.00	0.93	27	0.91	1.48	SE7:
18186+3143......	TU Lyr	Lb	...	M6	−0.92	0.92	22	0.50	1.16	SE4t
18213+0335......	V2090 Oph	Lb:	...	M6:–9	−1.36	0.85	28	1.05	1.44	SE6
18222+3933......	TW Lyr	M	376.71	M6	−0.55	0.66	41	0.48	0.93	SE1:t
18238−2542......	HO Sgr	M	437.00	M10	−1.00	0.61	28	1.12	1.41	SE6
18243+0352......	V988 Oph	SRb	...	M7e	−1.11	0.80	26	0.67	1.57	SE8t
18246−3321......	RV Sgr	M	315.85	M4e–9	−0.02	0.43	16	0.19	0.84	SE1:
18247+0729......	V585 Oph	SRb	135.00	M5	−0.11	0.84	15	0.29	0.93	SE1:
18296−0957......	VW Sct	M	234.00	M4–7	0.00	0.55	...	0.11	1.55	P:
18309−6955......	RT Pav	SRb	...	M4/5 III	−0.50	0.95	24	0.60	1.38	SE6:t
18347−0241......	CZ Ser	Lb	...	M6.5	−0.49	1.12	16	0.18	1.07	SE3:
18349+1023......	V1111 Oph	M	...	M4 III–9	−3.51	0.67	26	0.92	1.30	SE5
18359+0847......	X Oph	M	328.85	M5–9e	−2.90	0.44	15	0.24	0.94	SE1
18396−4549......	RW Tel	SRb	127.35	M4–6II–IIIe	−0.10	0.69	16	0.16	1.00	SE2:
18399−1920......	V3879 Sgr	SRb	...	M5.2 III	−1.17	0.18	18	−0.04	1.50	N
18401+2854......	FI Lyr	SRb	146.00	M	−1.30	0.98	41	0.62	1.00	SE2t
18406−4324......	V388 CrA	M:	...	Me	−0.75	0.76	29	1.32	1.54	SE7
18409+1220......	KX Her	M	495.00	M8e	−1.21	0.99	28	1.26	1.37	SE6
18429−1721......	V3952 Sgr	M:	...	M9	−0.90	1.03	29	1.57	1.47	SE7
18436+4334......	RW Lyr	M	503.75	M7e	−0.90	1.29	27	0.94	1.42	SE6
18494+1209......	LO Her	M	471.00	M8 III	−0.24	0.90	26	1.16	1.24	SE4:
18501−2132......	V2059 Sgr	M	405.00	M8	−0.91	0.93	23	0.56	1.19	SE4
18520−1635......	UX Sgr	SRb	100.00	Mb	−1.34	0.90	24	0.45	1.53	SE7
18537−1035......	RW Sct	SRb	116.70	M5	−0.68	0.42	17	0.07	0.88	SE1:
18537+4352......	R Lyr	SRb	...	M5 III	−2.79	0.12	...	0.02	0.69	N
18560−2954......	V3953 Sgr	M:	...	M9	−3.39	0.84	27	1.00	1.38	SE6
19007−2247......	SU Sgr	SRb	...	M6 III	−1.59	0.69	16	0.21	1.18	SE4t
19039+0809......	R Aql	M	284.20	M5–9e	−2.88	1.02	23	0.36	1.28	SE5
19042−4858......	U Tel	M	445.00	M7e	−2.15	1.03	29	1.31	1.44	SE6
19045+0704......	V844 Aql	SRa	369.00	M5–7ep	−0.50	0.40	16	0.14	1.03	SE2
19047−1706......	FQ Sgr	M	434.00	M8e	−1.19	0.66	41	0.45	0.96	SE2
19055+0613......	V347 Aql	Lb	...	M6–8	−1.37	0.57	15	0.24	0.92	SE1t
19059−2219......	V3880 Sgr	M	510.00	M8:	−2.53	1.22	28	1.20	1.30	SE5
19093−3256......	V342 Sgr	M	372.00	M9	−2.63	1.11	28	1.15	1.38	SE6
19098+6601......	SZ Dra	Lb	...	M5	−0.42	1.02	22	0.35	1.29	SE5
19118+4653......	SS Lyr	M	346.33	M5 IIIe	−0.28	0.64	14	0.40	1.04	SE2:
19143−5032......	V Tel	SRb	125.00	M6/8	−1.48	0.97	14	0.46	1.04	SE2t
19152−3640......	V924 Sgr	M	285.00	Me	−0.58	1.04	29	1.06	1.49	SE7t
19167−2101......	Z Sgr	M	450.41	M4e–9(Se)	−0.10	0.68	22	0.31	1.10	SE3:
19194+1734......	T Sge	SRb	165.50	M4−6.5	−1.74	0.74	15	0.36	1.05	SE3t
19243+7135......	YZ Dra	M	347.60	M8e	−0.58	0.69	24	0.63	1.29	SE5t
19267+0345......	V858 Aql	Lb	...	M4–5	−0.50	1.11	26	0.93	1.35	SE6
19287+4602......	AF Cyg	SRb	...	M5e–7	−1.10	0.68	16	0.20	1.06	SE3t
19296+4331......	UV Cyg	SRb	135.50	M6	−1.41	0.94	25	1.08	1.25	SE4t
19306+0455......	V1293 Aql	SRb	...	M5 III	−0.38	0.83	43	0.24	1.12	SE3:
19309−6252......	Z Pav	SRb	135.50	M7 IIIe	−0.89	0.54	16	0.13	0.90	SE1
19312+0521......	V450 Aql	SRb	...	M5 III–8 III	−0.81	0.09	17	−0.00	1.83	N:
19324+3033......	HR Cyg	M	561.00	M8–10	−0.30	0.90	26	0.90	1.29	SE5
19328+0035......	V607 Aql	M	474.00	M9	−0.46	0.85	25	0.82	1.35	SE5:
19356+1136......	RT Aql	M	327.11	M6–8e(S)	−1.05	0.75	24	0.56	1.29	SE5
19369+2823......	BG Cyg	M	288.00	M7–8e	−0.74	0.50	15	0.26	0.97	SE2t
19384+4346......	V462 Cyg	M	366.68	M7e	−0.11	0.63	14	0.35	0.62	SE1:
19409+5520......	V1351 Cyg	Lb	...	M5 IIIa	−0.32	0.17	18	−0.02	2.10	N
19440−4118......	V3960 Sgr	Lb	...	M5/7	−0.13	0.82	22	0.27	1.15	SE3:
19451+1824......	δ Sge	Lb:	...	M2.5 II–III+B9V	−1.39	0.06	18	−0.03	1.57	N
19503+2219......	NS Vul	Lb:	...	M5III	−2.26	0.80	24	0.61	1.33	SE5t
19510−5919......	S Pav	SRa	380.86	M7 IIe–8 III	−3.12	0.58	14	0.32	0.97	SE2t
19528−2919......	RR Sgr	M	336.33	M4–9e	−1.75	0.51	23	0.34	1.25	SE4
19536+3237......	V468 Cyg	M	485.80	M7	−1.38	1.05	28	1.04	1.43	SE6
19550−0201......	RR Aql	M	394.78	M6e–9	−2.67	0.70	27	0.85	1.50	SE7
19564−0801......	RS Aql	M	410.12	M5e–8	−0.12	0.47	14	0.47	1.05	SE2:
19575−5930......	NU Pav	SRb	...	M6 III	−2.28	0.07	18	0.00	0.29	N
19577+1722......	VZ Sge	Lb	...	M4 IIIa	−0.62	0.03	18	−0.04	1.10	N:
19586+3637......	V1511 Cyg	Lb	...	M10 III	−1.25	1.38	29	1.25	1.39	SE6
19595−2751......	V3872 Sgr	Lb	...	M4 III	−1.34	0.16	17	0.01	0.00	N
20000+4954......	Z Cyg	M	263.69	M5–9e	−1.14	1.35	69	1.09	1.58	SE8
20010+3011......	V718 Cyg	SRb	264.00	M0–5	−0.78	1.19	27	1.58	1.23	SE4t
20015+3019......	V719 Cyg	Lb	...	M4e	−1.90	1.19	29	2.17	1.26	SE5

TABLE 4—*Continued*

PSC (1)	Name (2)	Variability (3)	Period (d) (4)	Spectral Type (5)	[12] (6)	[12] − [25] (7)	LRS (8)	D.E.C. (9)	F_{11}/F_{12} (10)	Dust (11)
20038−2722......	V1943 Sgr	Lb	...	M8	−2.86	0.53	15	0.20	1.00	SE2t
20042+1040......	V466 Aql	M	428.00	M5	−0.37	0.47	28	1.08	1.39	SE6:
20047+1248......	SY Aql	M	355.92	M5–7e	−0.90	0.81	28	0.98	1.50	SE7t
20062+5650......	V555 Cyg	Lb	...	M5	−0.30	0.90	...	0.82	1.01	SE2:
20075−6005......	X Pav	SRb	199.19	Mc	−3.23	0.79	22	0.63	1.15	SE3t
20077−0625......	V1300 Aql	M:	680.00	M:	−4.12	1.38	23	0.79	0.99	SB
20079−0146......	V584 Aql	Lb	...	M8	−0.82	0.76	21	0.31	1.13	SE3t
20109+3205......	V557 Cyg	M	382.00	M7–9	−0.75	1.00	29	1.11	1.51	SE7
20113+4917......	AC Cyg	SRb	142.00	M7	−1.37	0.89	24	0.55	1.41	SE6t
20125+0856......	R Del	M	285.07	M5–6e	−0.10	0.52	15	0.29	1.12	SE3:
20135+3055......	SX Cyg	M	411.02	M7e	−0.17	0.71	21	0.38	1.01	SE2:
20144−3916......	RT Sgr	M	306.46	M5–7e	−0.42	0.43	16	0.25	1.09	SE3:
20165+3413......	AU Cyg	M	435.31	M6–7e	−1.40	0.94	27	0.99	1.41	SE6
20165−5051......	Y Tel	Lb	...	M7 III	−0.89	0.73	16	0.18	0.98	SE2
20198+4017......	V405 Cyg	Lb	...	M6.5	−0.34	0.75	21	0.22	1.23	SE4:t
20198+6843......	AC Dra	Lb	...	M5 IIIab	−0.71	0.11	18	0.01	0.00	N
20239+2604......	AV Vul	Lb	...	M5–8	−0.06	1.01	22	0.58	1.23	SE4:
20248−2825......	T Mic	SRb	347.00	M6e	−3.10	0.53	15	0.20	0.94	SE1t
20248+7505......	UU Dra	SRb	120.00	M8 IIIe	−1.67	1.14	23	0.74	1.20	SE4t
20255+4054......	KZ Cyg	M	405.95	M8e	−0.39	0.68	21	0.35	1.11	SE3
20259−4035......	U Mic	M	334.29	M5–7e	−0.15	0.87	24	0.51	1.49	SE7
20268+1606......	RS Del	SRb:	...	M5–8	−0.55	0.51	17	0.11	1.02	SE2
20270+0943......	CT Del	Lb	...	M7	−0.05	0.65	23	0.23	1.56	SE8:
20276−0455......	TZ Aql	Lb	...	M6	−0.47	1.06	...	0.55	1.66	SE8:
20296−2151......	RU Cap	M	347.37	M9e	−0.14	1.09	28	0.95	1.60	SE8
20297+3221......	AI Cyg	SRb	197.30	M6–7	−0.15	0.97	23	0.41	1.28	SE5:
20305+6246......	BF Cep	M	430.14	M7	−0.06	0.54	16	0.19	0.89	SE1:
20356+1805......	EU Del	SRb	...	M6.4 III	−1.98	0.17	17	0.03	0.22	N
20392+1141......	Y Del	M	468.40	M8e	−0.29	1.00	23	0.57	1.18	SE4t
20417−0500......	Y Aqr	M	382.34	M6.5e–9	−0.44	0.64	23	0.52	1.21	SE4:
20425+3218......	V570 Cyg	M	500.00	M5–7	−0.62	1.03	28	1.14	1.34	SE5
20431+1754......	U Del	SRb	110.00	M5 II–III	−1.75	0.91	23	0.40	1.29	SE5t
20438−0415......	W Aqr	M	381.10	M6–8e	−0.89	0.55	22	0.34	1.14	SE3
20443+0215......	V Aqr	SRa	244.00	M6e	−0.97	0.43	...	0.18	0.98	SE2:
20451−0512......	EN Aqr	Lb	...	M3 III	−0.82	0.04	18	−0.02	0.00	N
20466+2248......	FI Vul	Lb	...	M3	−0.82	0.37	16	0.11	1.26	SE5:
20469+3139......	AM Cyg	M	370.60	M6e	−0.28	0.63	...	0.33	1.08	SE3:
20502+4709......	RZ Cyg	SRa	275.69	M7.0–8.2ea	−1.42	0.99	23	0.78	1.12	SE3t
20503+2658......	UW Vul	M	365.50	M7	0.00	0.62	14	0.44	1.01	SE2:
20507+2310......	RX Vul	M	457.00	M9e	−1.01	0.73	13	0.60	1.00	SE2t
20511+2523......	IN Vul	Lb	...	M7	−0.21	0.83	14	0.30	0.99	SE2:t
20526−5431......	S Ind	M	399.95	M6–8e II–Ib:	−0.78	0.99	22	0.29	1.25	SE5
20529+3013......	UX Cyg	M	565.00	M4–6.5e	−1.96	0.99	29	1.41	1.56	SE8t
20581+5841......	UW Cep	M	...	M8	−0.04	0.80	22	0.57	1.13	SE3:
21012+2347......	DY Vul	Lb	...	M3–6	−0.83	0.19	18	−0.01	1.28	N
21044−1637......	RS Cap	SRb	340.00	M4	−2.27	0.80	27	0.71	1.53	SE7t
21088+6817......	T Cep	M	388.14	M5.5–8.8e	−3.56	0.43	15	0.22	0.94	SE1
21100−1435......	RX Aqr	Lb:	...	M4	−0.87	0.67	24	0.31	1.54	SE7
21206−4054......	V Mic	M	381.15	M3–6e	−1.57	1.08	29	1.12	1.46	SE7
21208+7737......	GH Cep	M	331.00	M3	−1.00	0.77	26	0.75	1.40	SE6
21243−6943......	SX Pav	SRb	...	M5–7 III	−1.49	0.11	18	−0.00	0.00	N
21286+1055......	UU Peg	M	456.50	M7e	−1.89	1.11	26	0.93	1.32	SE5
21341+4508......	W Cyg	SRb	131.10	M4–6e(Tc:) III	−2.73	0.59	16	0.13	1.03	SE2
21389+5405......	RU Cyg	SRa	233.43	M6–8e	−2.07	0.92	24	0.62	1.32	SE5t
21402+4532......	V1339 Cyg	SRb	...	M3–6	−0.46	0.16	...	0.01	0.83	N:
21414+7609......	AM Cep	M	333.00	M8	−0.56	0.81	14	0.48	0.99	SE2
21426+1228......	TU Peg	M	321.60	M7–8e	−0.81	0.69	15	0.32	0.99	SE2
21439−0226......	EP Aqr	SRb	...	M8 III	−3.38	0.81	23	0.52	1.28	SE5t
21453−4708......	R Gru	M	331.96	M5–7 II–IIIe	−0.25	0.62	15	0.27	0.86	SE1:
21456+6422......	RT Cep	M	621.55	M6	−1.98	1.04	28	1.27	1.33	SE5
21563+5630......	PR Cep	Lb:	...	M8	−1.19	1.03	26	0.89	1.28	SE5
21565+4132......	DL Lac	M	375.00	Me	−0.72	1.04	...	1.56	1.59	SE8
22000+5643......	YY Cep	M	526.08	M6	−0.40	0.63	23	0.60	1.18	SE4
22017+2806......	TW Peg	SRb	929.30	M6−8	−2.42	0.97	26	0.83	1.43	SE6t
22023+6252......	MO Cep	Lb:	...	M5 III	−0.58	0.07	17	0.04	0.70	N
22035+3506......	SV Peg	SRb	144.60	M7	−2.43	0.92	21	0.49	1.10	SE3t
22097+5647......	CU Cep	SRb	700.00	M4–6	−2.14	1.12	29	1.64	1.41	SE6t
22142−8454......	BW Oct	Lb:	...	M7 III	−1.76	0.82	23	0.41	1.26	SE5t
22145−8041......	ϵ Oct	SRb	...	M6 III	−1.81	0.12	...	0.00	0.00	N
22230−4841......	S Gru	M	401.51	M5–8IIIe	−1.64	0.69	22	0.37	1.19	SE4
22233+3013......	RV Peg	M	396.80	M6e	−1.60	0.97	29	1.76	1.51	SE7
22267−4400......	δ Gru	Lb:	...	M4.5 IIIa	−1.47	0.07	18	−0.01	0.00	N

TABLE 4—*Continued*

PSC (1)	Name (2)	Variability (3)	Period (d) (4)	Spectral Type (5)	[12] (6)	[12] − [25] (7)	LRS (8)	D.E.C. (9)	F_{11}/F_{12} (10)	Dust (11)
22272+5435......	V354 Lac	Lb	...	M0 III:	−1.04	3.09	72	1.81	0.49	H
22280+1250......	GM Peg	Lb	...	M8	−0.32	0.54	15	0.27	1.02	SE2:
22296−6214......	ν Tuc	Lb:	...	M4 III	−0.82	0.06	18	−0.05	1.32	N
22306+5510......	NY Lac	SRb	150.00	M7.5–8	−0.60	0.86	21	0.41	1.07	SE3
22315+2418......	SS Peg	M	424.80	M6–7e	−1.20	0.35	14	0.30	0.95	SE2:t
22359−1417......	AB Aqr	Lb	...	M7	−0.35	0.85	15	0.29	0.95	SE2t
22466+2705......	ST Peg	SRb	136.20	M6e	−0.51	0.81	...	0.32	1.31	SE5:
22476+4047......	RX Lac	SRb	650.00	M7.5Se	−1.36	0.36	16	0.12	0.85	SE1
22489+6359......	VX Cep	M	532.30	M8	−0.54	0.76	22	0.40	1.05	SE3:
22525−2952......	V PsA	SRb	148.00	Mb	−2.35	0.69	22	0.35	1.24	SE4t
22586+4614......	BC And	Lb	...	M7 III	−0.02	0.83	...	0.19	1.08	SE3:
22594+6117......	V352 Cep	Lb	...	M7:	−0.16	1.13	25	0.35	1.91	SE8:t
23000+5932......	AS Cep	Lb	...	M3	−0.73	1.16	28	1.70	1.34	SE5t
23013+2748......	β Peg	Lb	...	M2.5 II–IIIe	−2.84	0.06	18	−0.01	1.08	N
23013+3735......	CF And	Lb	...	M7	−1.46	0.93	...	1.03	1.38	SE6t
23041+1016......	R Peg	M	378.10	M6–9e	−2.03	0.57	22	0.41	1.18	SE4
23063−3024......	Y Scl	SRb	...	M4	−1.49	0.62	...	0.54	1.52	SE7
23070+0824......	GZ Peg	SRa	...	M4S III	−1.14	0.05	18	−0.01	0.00	N:
23093+4843......	ES And	Lb	...	M6	−0.11	0.89	15	0.29	1.01	SE2:
23095+5925......	V Cas	M	228.83	M5–8.5e	−0.94	0.47	16	0.13	0.83	SE1
23106+6340......	CK Cep	SRb	110.00	M7	−0.09	0.74	15	0.22	0.93	SE1:
23142−0759......	χ Aqr	Lb	...	M3 III	−0.90	0.10	...	0.00	0.00	N
23142+1019......	EO Peg	Lb	...	M7	−0.38	0.11	17	0.06	0.76	N:
23173+2600......	W Peg	M	345.50	M6–8e	−2.22	0.65	...	0.37	1.13	SE3
23173+4823......	BE And	SRb	...	M5	−0.26	0.47	15	0.26	1.09	SE3:t
23180+0838......	S Peg	M	319.22	M5–8.5e	−0.37	0.44	...	0.18	0.93	SE1:t
23182+3920......	RY And	M	393.40	M8	−0.19	0.77	24	0.66	1.22	SE4:
23201−1105......	SV Aqr	Lb	...	Mb	−0.57	0.79	15	0.28	1.03	SE2:
23202+5901......	V398 Cas	Lb	...	M2	−0.77	0.55	22	0.34	1.15	SE4
23212+3927......	BU And	M	382.15	M7e	−1.41	0.67	14	0.44	1.01	SE2
23278+6000......	V582 Cas	SRa	300.00	M5	−1.39	1.24	...	1.33	1.32	SE5
23284+5958......	V530 Cas	Lb	...	M3	−1.65	1.22	29	1.79	1.39	SE6
23309+2213......	HW Peg	Lb:	...	M5 IIIa	−0.86	0.07	18	−0.02	1.12	N:
23365+5159......	SV Cas	SRa	264.50	M6.5	−1.64	1.06	25	0.71	1.39	SE6
23412−1533......	R Aqr	M	386.96	M5–8.5e+peC	−4.37	0.40	...	0.36	1.46	SE7
23420+5618......	Z Cas	M	495.71	M7e	−0.97	0.97	41	0.46	0.93	SE1
23425+4338......	EY And	M	360.00	M7–9	−1.02	1.25	26	0.95	1.35	SE5
23439+5412......	RT Cas	SRa	399.80	M7	−0.36	0.65	15	0.30	0.90	SE1
23522−0010......	XZ Psc	Lb	...	M5IIb	−0.50	0.08	18	−0.01	0.79	N:
23528+4821......	RS And	SRa	136.00	M7–10	−1.59	0.70	22	0.37	1.30	SE5t
23558+5106......	R Cas	M	430.46	M6–10e	−4.19	0.60	24	0.61	1.27	SE5t
23564−5651......	S Phe	SRb	141.00	M3–6 IIIe	−1.13	0.80	02	0.51	1.98	SE8
23575+2536......	Z Peg	M	334.80	M6–8.5e(Tc)	−0.70	0.62	15	0.25	0.89	SE1:
23594−0617......	YY Psc	Lb:	...	M3 III	−1.22	−0.11	18	−0.04	0.70	N

siders the Mira variables and expands the comparison to supergiants and S stars, where differences in the distribution of dust types do occur.

3.1. *The Light Curve of Mira Variables*

Among Mira variables, the spectrum from oxygen-rich dust varies with the shape of the light curve (Vardya, de Jong, & Willems 1986). Mira variables with asymmetric light curves tend to show classic silicate emission while Mira variables with more symmetric light curves generally show the broad emission feature. The silicate dust sequence allows a more quantitative analysis of this relationship, as Figure 5 shows by plotting the asymmetry factor ($f = 100 \times$ rise time/total period) as a function of corrected flux ratio F_{11}/F_{12} (which is the basis for the SE index in eq. [5]). A least-squares fit over the range SE1–7 (i.e., 0.85 $< F_{11}/F_{12} <$ 1.55) gives $f = 62 - 16.5 \times F_{11}/F_{12}$ with a correlation coefficient of 0.58.

3.2. *Supergiants*

The supergiants are divided into two variability classes, SRc and Lc. The irregulars (Lc) pulsate too weakly for any

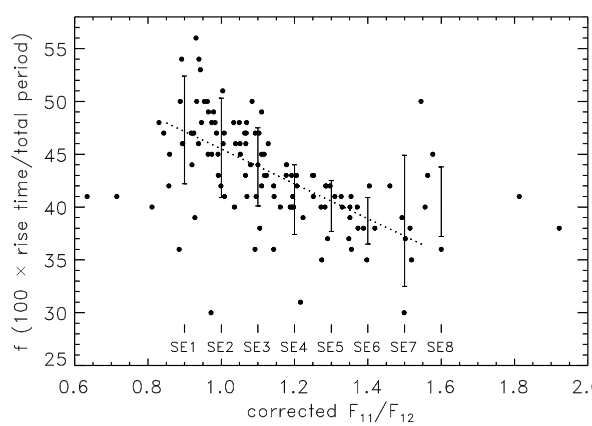

FIG. 5.—Relationship between the shape of the silicate feature (*horizontal axis*) and the asymmetry of the light curve for the Mira variables in our sample. Mira variables with symmetric light curves tend to show broad emission (SE1–3), while Mira variables with the most asymmetric light curves tend to have features classified as SE5–7 (structured and classic silicate profiles). The dashed line is a least-squares fit over the SE1–7 range.

TABLE 5

INFRARED SPECTRAL CLASSIFICATIONS OF THE SUPERGIANTS

PSC (1)	Name (2)	Variability (3)	Period (d) (4)	Spectral Type (5)	[12] (6)	[12]−[25] (7)	LRS (8)	D.E.C. (9)	F_{11}/F_{12} (10)	Dust (11)
00192−2020	T Cet	SRc	158.90	M5–6S IIe	−2.11	0.19	16	0.15	0.76	SE1t
01597+5459	XX Per	SRc	415.00	M4 Ib+b	−1.00	0.57	26	0.66	1.47	SE7
02153+5711	BU Per	SRc	367.00	M3.5 Ib	−0.50	1.17	29	1.47	1.48	SE7
02185+5622	SU Per	SRc	533.00	M3.5 Iab	−0.59	1.06	25	0.81	1.28	SE5
02188+5652	RS Per	SRc	244.50	M4 Iab	−1.05	1.08	26	1.09	1.33	SE5t
02192+5821	S Per	SRc	822.00	M3 Iae–7	−2.70	1.15	26	1.53	1.20	SE4t
02384+3418	W Tri	SRc	108.00	M5 II	−0.45	0.80	23	0.40	1.26	SE5
02469+5646	W Per	SRc	485.00	M3 Ia–Iab–7	−1.26	1.41	28	1.68	1.30	SE5t
03030+5532	IO Per	Lc	…	M3 Iab	−2.32	1.28	27	1.28	1.32	SE5t
03113+5441	V411 Per	SRc	467.00	M3.4 Ia	−0.25	1.22	14	0.58	1.14	SE3
03449+6522	BE Cam	Lc	…	M2 II	−1.31	0.15	18	−0.00	0.00	N
04020−1551	V Eri	SRc	…	M6 II	−2.65	0.94	22	0.67	1.08	SE3t
05292+1833	CE Tau	SRc	165.00	M2 Iab–Ib	−1.77	0.32	17	0.01	0.00	N
05374+3153	NO Aur	Lc	…	M2S Iab	−0.47	0.86	43	0.23	0.92	SE1
05524+0723	α Ori	SRc	128.14	M1–2 Ia–Ibe	−5.55	0.48	02	0.25	1.79	SE8
05562+4556	π Aur	Lc	…	M3.5 II	−1.45	0.08	18	0.01	0.00	N
06088+2152	TV Gem	SRc	…	K5.5–M1.3 Iab	−1.33	0.64	28	1.03	1.43	SE6
06092+2255	BU Gem	Lc	…	M1–2 Ia–Iab	−1.10	1.02	23	0.67	1.23	SE4t
06210+4918	ψ Aur	Lc	…	K5–M0 Iab–Ib	−0.48	0.66	21	0.15	1.24	SE4
06520−2407	o CMa	Lc	…	K2.5 Iab	−0.35	0.53	17	0.04	0.79	N
06597−2751	σ CMa	Lc	…	K7 Ib	−1.09	0.18	…	0.04	0.48	N
07245+4605	Y Lyn	SRc	110.00	M6S Ib–II	−1.59	0.86	23	0.29	1.35	SE6
07314−1424	KQ Pup	Lc	…	M2ep–Iab+B2–V	−0.66	0.12	18	−0.01	0.00	N
08023−3231	MZ Pup	Lc:	…	M1–IIb	−0.51	0.31	17	0.03	0.50	N
08372−0924	RV Hya	SRc	116.00	M5–II	−1.08	0.86	24	0.46	1.39	SE6
09076+3110	RS Cnc	SRc:	120.00	M6e–Ib–II(S)	−3.07	0.66	22	0.25	1.44	SE6t
10056−5300	CM Vel	SRc	780.00	M0–5(II)	−2.94	0.97	29	2.45	1.45	SE7t
10154−6104	V337 Car	Lc	…	K3 II	−0.57	−0.03	18	−0.05	1.40	N
10186−6012	EV Car	SRc	347.00	M4.5 Ia	−2.43	1.04	29	1.94	1.42	SE6
10226−5956	CK Car	SRc	525.00	M3.5 Iab	−1.51	1.04	29	2.02	1.43	SE6
10428−5909	RT Car	Lc	…	M2 Ia–0	−1.20	1.72	…	3.41	1.30	H(SE)
10484−5943	IX Car	SRc	400.00	M2 Iab	−0.66	1.21	27	1.07	1.40	SE6
10520−6049	CL Car	SRc	513.00	M5 Iab	−1.02	0.75	26	0.90	1.30	SE5
13141−6119	V396 Cen	Lc:	…	M4 Ia–Iab–6	−0.69	1.24	25	0.68	1.35	SE5
16262−2619A	α Sco	Lc	…	M1.5 Iab–Ib	−5.13	−0.11	…	0.06	2.73	SE8
17080−3215	AH Sco	SRc	713.60	M4e–5 Ia–Iab	−3.37	0.92	28	1.58	1.33	SE5t
17123+1426	α Her	SRc	…	M5 Ib–II	−4.32	0.19	19	−0.04	0.93	N
17488−2800	KW Sgr	SRc	670.00	M0 I–4Ia	−2.37	0.99	29	1.55	1.38	SE6
17566−3555	V540 Sgr	Lc	…	M5 Iab	−0.76	1.04	29	1.33	1.43	SE6
18050−2213	VX Sgr	SRc	732.00	M4 Ia–10eIa	−4.96	0.82	26	0.73	1.41	SE6
18248−1229	UY Sct	SRc	740.00	M4 Ia–Iab	−2.41	1.25	…	1.64	1.21	SE4
18364+3937	XY Lyr	Lc	…	M4–5 Ib–II	−1.07	0.14	17	0.05	1.00	SE2
18527+3650	δ Lyr	SRc:	…	M4 II	−1.85	0.20	18	0.01	0.98	N
18550+0023	UW Aql	Lc	…	M0 Iab–2Ia–Iab	−0.07	0.80	24	0.50	1.28	SE5
19032−4602	RX Tel	SRc	349.60	M3 Iab	−1.37	1.09	29	2.36	1.52	SE7
19480+2447	NR Vul	Lc	…	M1 Ia	−1.44	0.92	26	1.21	1.24	SE4
20193+3527	V1749 Cyg	Lc	…	M3 Iab	−0.42	1.11	23	0.65	1.12	SE3t
20194+3646	BI Cyg	Lc	…	M4 Iab	−2.68	1.22	29	1.87	1.44	SE6
20197+3722	BC Cyg	SRc	700.00	M3.5 Ia	−2.94	2.71	…	1.44	1.30	H(SE)
20241+3811	KY Cyg	Lc	…	M3.5 Ia	−3.14	1.08	…	1.62	1.26	SE5
20270+3948	RW Cyg	SRc	550.00	M2–4 Ia–Iab	−2.56	1.07	…	1.36	1.36	SE6
21245+6221	SW Cep	SRc	…	M3.5 Ia–Iab	−1.10	1.25	29	1.91	1.42	SE6t
21417+0938	ϵ Peg	Lc	…	K2 Ib	−1.41	0.01	18	−0.01	0.00	N
21419+5832	μ Cep	SRc	730.00	M2e Ia	−4.15	0.74	28	0.74	1.60	SE8
21552+6323	VV Cep	EA/GS+SRc	430.00	M2p Ia–Iab+B8:e V	−0.99	0.27	17	−0.00	0.00	N
22282+5644	ST Cep	Lc	…	M2 Ia–Iab	−0.72	1.10	28	1.29	1.49	SE7
22317+5838	V354 Cep	Lc	…	M2.7 Iab	−1.10	1.00	29	1.75	1.39	SE6
22345+5809	W Cep	SRc	…	K0p–M2ep Ia+B0/B1	−1.58	1.20	29	1.19	1.50	SE7
22396−4708	β Gru	Lc:	…	M3–5 II–III	−3.81	0.06	…	0.01	1.04	N
22456+5453	U Lac	SRc	…	M4ep Iab+b	−1.60	0.80	27	0.81	1.45	SE7
22525+6033	MY Cep	SRc	…	M7–7.5I	−1.49	1.35	24	1.14	1.11	SE3
23092+5236	SS And	SRc	152.50	M6 II	−0.50	0.66	16	0.19	0.76	SE1
23281+5742	V358 Cas	Lc	…	M3 Ia–Iab	−1.18	1.36	29	2.40	1.42	SE6t
23416+6130	PZ Cas	SRc	925.00	M2–4 Ia	−2.80	1.63	69	1.93	1.37	SE6
23504+6043	TZ Cas	Lc	…	M2 Iab	−1.06	1.16	29	1.55	1.48	SE7

TABLE 6

INFRARED SPECTRAL CLASSIFICATIONS OF THE OPTICAL S STARS

PSC (1)	Name (2)	Variability (3)	Period (d) (4)	Spectral Type (5)	[12] (6)	[12]−[25] (7)	LRS (8)	D.E.C. (9)	F_{11}/F_{12} (10)	Dust (11)
00001+4826......	IW Cas	M	396.38	S4.5,9e	−0.59	0.79	21	0.39	1.08	SE3
00213+3817......	R And	M	409.33	S3,5–8,8e(M7e)	−2.66	0.83	...	0.70	1.09	SE3
00428+6854......	V524 Cas	M	...	S	−1.00	1.20	27	1.17	1.26	SE5
01159+7220......	S Cas	M	612.43	S3,4–5,8e	−2.71	0.95	22	0.53	1.07	SE3
03377+6303......	BD Cam	Lb	...	S5,3(M4 III)	−0.40	0.11	18	−0.03	1.04	N
04352+6602......	T Cam	M	373.20	S4,7–8.5,8e	−0.41	0.21	17	0.03	0.57	N
10436−3459......	Z Ant	SR	103.80	S5,4	−0.08	0.73	42	0.55	0.85	SE1
13136−4426......	UY Cen	SR	114.60	SC	−0.72	0.49	43	0.14	1.07	SiC
13477−6009......	VX Cen	SR	307.80	S8,5e(M4–8II–III)	−0.54	0.27	17	0.06	0.68	SE1:
16334−3107......	ST Sco	SRa	194.50	S4,7:(R5)	−0.66	0.63	16	0.21	0.88	SE1
17206−2826......	V521 Oph	SRb	320.00	S5,4(M4)	−0.33	0.28	17	0.02	0.00	N
17544−2951......	V1717 Sgr	SRa	440.00	Ce:(K5)	−1.03	0.91	41	0.27	0.97	SE2
18586−1249......	ST Sgr	M	395.12	C4,3–S9,5e	−0.67	0.48	21	0.24	1.12	SE3
19111+2555......	S Lyr	M	438.40	SCe	−0.43	0.76	41	0.33	1.01	SE2
19126−0708......	W Aql	M	490.43	S3,9–6,9e	−4.36	0.63	22	0.37	1.10	SE3
19133−1703......	T Sgr	M	394.66	S4.5,8–5.5,8e	−0.38	0.44	...	0.16	0.91	SE1
19311+2332......	EP Vul	Lb	...	S6,5–8,7	−0.12	0.66	16	0.12	0.39	SiC
19354+5005......	R Cyg	M	426.45	S2.5,9–6,9e(Tc)	−1.42	0.80	22	0.34	1.08	SE3
19486+3247......	χ Cyg	M	408.05	S6,2–10,4e(MSe)	−4.44	0.15	...	0.28	1.07	SE3
20026+3640......	AA Cyg	SRb	212.70	S7,5–7.5,6(MpTc)	−0.37	0.54	31	0.07	0.00	N
20120−4433......	RZ Sgr	SRb	223.20	S4,4ep	−0.33	1.10	16	0.22	0.98	SE2
21027+3704......	GR Cyg	M	...	S	−1.28	0.56	...	0.31	0.76	SiC
22196−4612......	π Gru	SRb	150.00	S5,7e	−3.77	0.77	42	0.31	1.00	SE2
23554+5612......	WY Cas	M	476.56	S6,5pe	−0.64	0.93	42	0.41	1.07	SE3

characteristic period to emerge and are analogous to Lb variables on the AGB. The SRc variables pulsate with enough regularity for a period to be identified; they probably pulsate in an overtone mode (or two), while Lc variables pulsate in a series of higher overtones. Hoffmeister et al. (1984) point out that most or all of the red supergiants not yet identified as variables are probably low-amplitude irregulars.

The percentage of naked stars reflects the strength of the pulsation mode (Table 3). About one-third of the irregulars are naked, but only 10% of the semiregulars are. This behavior parallels the decreasing percentage of naked AGB stars along the sequence Lb → SRb → SRa → Mira (Paper I).

Varying the assumed photospheric continuum will rarely change the SE classification by more than one index, but we have still tried to reduce systematic errors by modifying our assumed spectrum for the differing samples. Table 7 shows the corresponding effective temperatures (Lang 1992) and percentage of SiO absorption (at the resolution of the LRS) used to define the stellar photospheres of the different samples, based on the mean spectral types of M4 for SRc variables and M2 for Lc variables.

One SRc (α Her) and one Lc (α Sco) appear to have *no* SiO absorption in the large LRS beam. A ground-based spectrum of α Her obtained with GLADYS at the Wyoming Infrared Observatory (WIRO) in 1993 (March 4 and June 27) shows an impressive 25% SiO absorption band from a smaller 2″ beam (Fig. 6), supporting the likelihood that low-level extended emission in the larger LRS beam has filled in the absorption feature (M. Cohen, private communication). The GLADYS spectrum was obtained using standard techniques described by Sloan, Grasdalen, & LeVan (1993) and calibrated with α Boo as a standard, using the template spectrum from Walker & Cohen (1992). Fitting and removing an Engelke function with no SiO absorption from the LRS spectra reveals that α Her is naked and that α Sco is a classic SE source.

TABLE 7

PROPERTIES OF PHOTOSPHERES

Subsample	Spectral Type	$T_{\rm eff}$ (K)	SiO Absorption (%)
AGB	M6 III	3240	15
S star......	M6 III	3240	15
SRc........	M4 I	2980	12
Lc	M2 I	3450	10

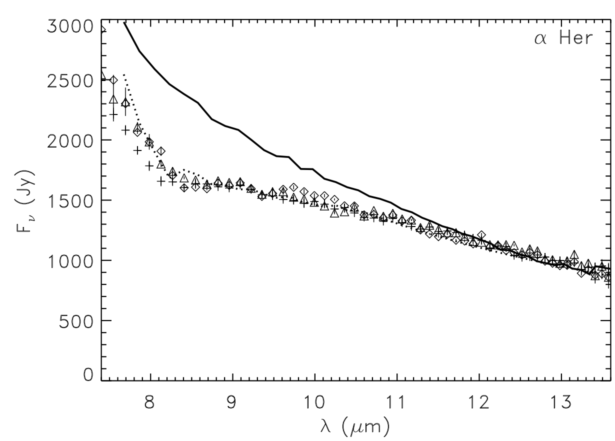

FIG. 6.—Three spectra of α Her from GLADYS (*symbols with error bars*), compared to the spectrum from the LRS (*solid line*), and a model spectrum (*dotted line*). The model is a 2800 K Engelke function, with 25% peak SiO absorption subtracted. Apparently, diffuse SiO molecular emission in the broad LRS beam has filled the photospheric absorption feature visible in the smaller GLADYS beam back in.

TABLE 8

PROPERTIES OF THE SUBSAMPLES

Variable	Total	SE Sources	⟨SE⟩	$\langle F_{11}/F_{12}\rangle$[a]	⟨D.E.C.⟩[b]	⟨[12]−[25]⟩
Lb	119	67	4.6 ± 2.4	1.21 ± 0.24	0.62 ± 0.58	0.86 ± 0.24
SRb	157	126	4.3 ± 2.3	1.18 ± 0.23	0.38 ± 0.27	0.76 ± 0.20
SRa.......	29	28	4.4 ± 3.0	1.19 ± 0.30	0.51 ± 0.37	0.76 ± 0.28
Mira......	241	232	4.6 ± 2.0	1.21 ± 0.21	0.61 ± 0.36	0.73 ± 0.22
Lc	27	17	5.4 ± 1.8	1.37 ± 0.38	1.02 ± 0.70	0.93 ± 0.39
SRc.......	38	33	5.9 ± 1.7	1.34 ± 0.20	1.11 ± 0.65	0.97 ± 0.29
MS	19	15	2.9 ± 1.9	1.08 ± 0.22	0.42 ± 0.57	0.67 ± 0.22
S..........	24	17	2.4 ± 1.1	1.01 ± 0.13	0.39 ± 0.25	0.73 ± 0.28

[a] Corrected flux ratio.
[b] Dust emission contrast.

Removing the stellar photosphere from the supergiant spectra reveals a distribution of SE classes significantly different from the AGB population (Fig. 7). Most of the supergiants fall into the range SE5–7, with more classic than structured silicate emission, compared to the AGB sources, which cover a much broader range of SE classes. The SRc variables are shifted slightly to more classic silicate emission than the Lc variables, but the difference of only half an SE index is not very meaningful given the large standard deviations of the sample (Table 8).

Most of the variable supergiants in this sample are distinguished from variable AGB sources by their optical spectral class. Many AGB sources, however, can have sufficiently low atmospheric pressures to mimic supergiants, but they will have much later spectral classes. Separating sources with spectral classes later than M4 in Figure 7 makes the difference between SRc variables and the AGB sample even larger.

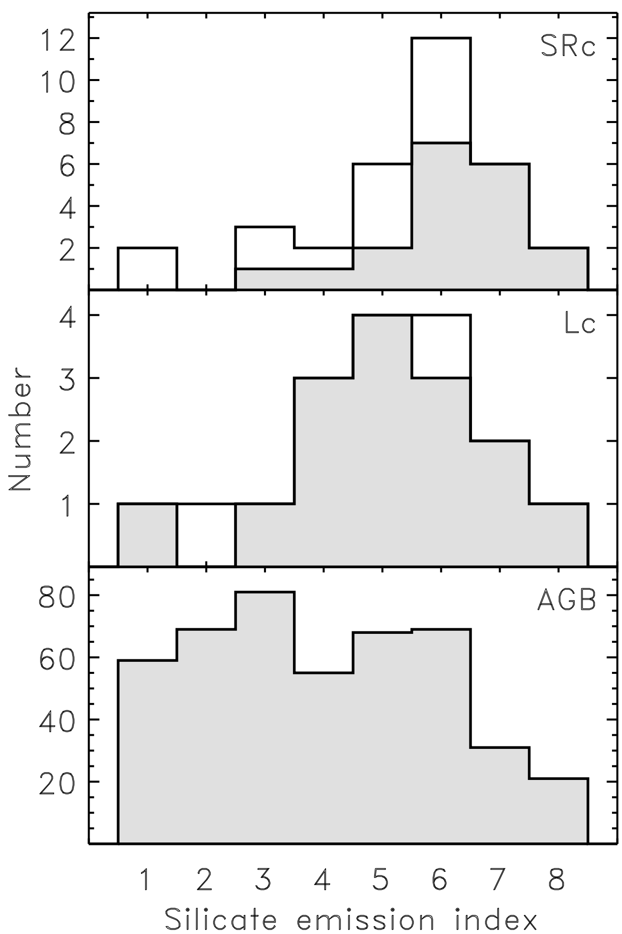

FIG. 7.—Distributions of silicate profile shapes for supergiants and the AGB sample. Neither the SRc nor the Lc samples contain many sources with broad emission (SE1–3). In the top two panels, the unshaded parts of the histogram count stars with spectral classes later than M4; these sources probably have lower mass than the other supergiants, may be on the AGB, and account for many of the broad emission spectra.

3.3. *S Stars*

To supplement our meager total of 24 S stars, we have borrowed 19 MS stars from the other samples, 15 from the oxygen-rich AGB sample, and four from the supergiant sample (listed in Table 9).

We assume the S stars have photospheric properties which are identical to the AGB sample (Table 7). Only four are naked. Three show carbon-rich emission (CE), and all of these would be classified as "SiC" sources in the system of Sloan et al. (1998). The remaining 17 show oxygen-rich dust emission (SE), and all but one show broad SE emission (SE1–3) (Fig. 8). Thus, the dust emission around S stars differs from the AGB sample as much as the supergiant sample, but in the opposite direction. Furthermore, not one of the S stars exhibited a 13 μm feature.

The MS stars appear to be a blend of S stars and normal oxygen-rich AGB sources. Four are naked; the remaining 15 are SE. Again, these concentrate in the SE1–3 range, although five lie in the SE4–6 range. Two of this latter group are from the supergiant sample, which tends to exhibit classic emission. The fraction of 13 μm sources among this group matches the fraction among the general AGB sample.

TABLE 9

MS STARS

AGB Sample	AGB Sample	AGB Sample
00445+3324	16496+1501	00192−2020
02143+4404	17001−3651	05374+3153
04497+1410	17553+4521	07245+4605
09564−5837	19167−2101	09076+3110
13144−6225	19356+1136	
13269−2301	22489+6340	
15492+4837	23070+0824	

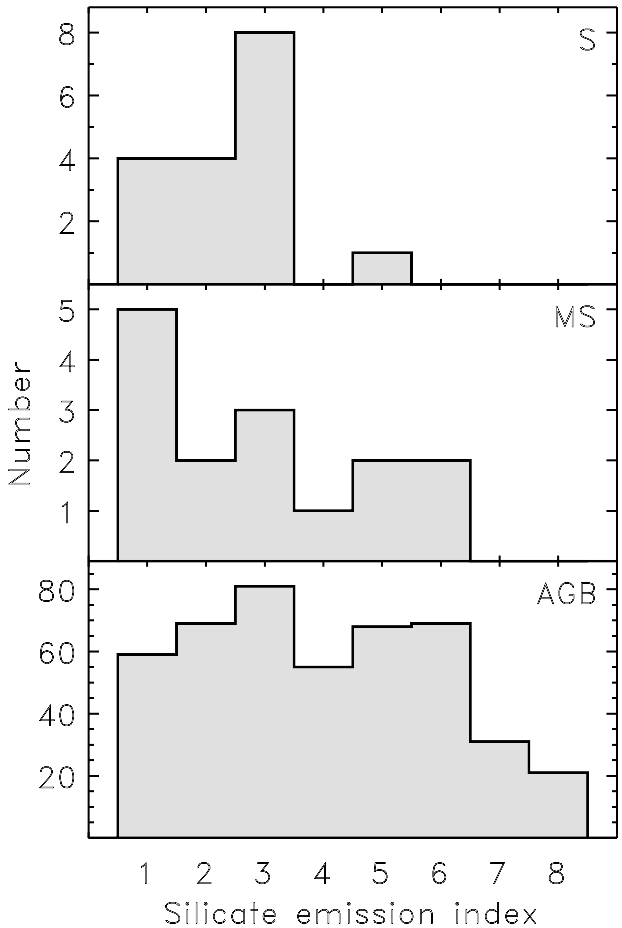

FIG. 8.—Distributions of silicate profile shapes for S stars, MS stars, and the AGB sample. All but one of the S stars show broad emission (SE1–3). The MS stars appear to be a blend of the S stars and AGB sample.

3.4. *The LML S Dust Class*

The LML classification method included a group of spectra in which the dust emission peaked in the 10.5–10.8 μm range. Little-Marenin & Little (1988) identified this group as the "S" class, and they suspected that the dust chemistry might be related to the unusual photospheric chemistry of S and MS stars. Paper I showed that the "S" class dust spectra generally fell in the SE3 portion of the silicate dust sequence, overlapping the Sil++ and three-component classes. Because of this overlap, Paper I called into question the existence of the "S" class as a distinct dust emission class but noted that flux ratios at 10, 11, and 12 μm were not very sensitive to fine-scale spectral details that might distinguish the "S" class spectra.

To look more carefully at the spectral properties of the "S" class in the LML system, we concentrate on those sources classified as "S" by LML and SE3 by us, and we compare their spectra to the average SE3 spectrum. Our AGB sample includes 16 of the 31 strong S stars examined by Little-Marenin & Little (1988). LML classified seven as "S," and six of these seven are classified here as SE3. Of the 11 Mira variables classified by Little-Marenin & Little (1990) as "S" that are in our AGB sample, six are SE3. Figure 9 compares the average spectra from these two groups to the sum of all SE3 sources in our AGB sample. The Mira variables and the SE3 sum are nearly indistinguishable. The spectrum from the S stars shows two differences from the SE3 sum. First, there is no 13 μm feature, since, as noted in the previous section, S stars do not exhibit this feature. Second, there is a slight enhancement in the dust emission from 10 to 11 μm, although its significance is questionable. Spectroscopic observations with the Short Wavelength Spectrometer aboard the *Infrared Space Observatory* (see, e.g., the STARTYP project by Price et al.) will permit analysis at higher spectral resolutions. At the resolution of the LRS, the only significant difference between the SE3 class in our system and the "S" class dust emission in the LML system is the lack of a 13 μm feature in the S stars.

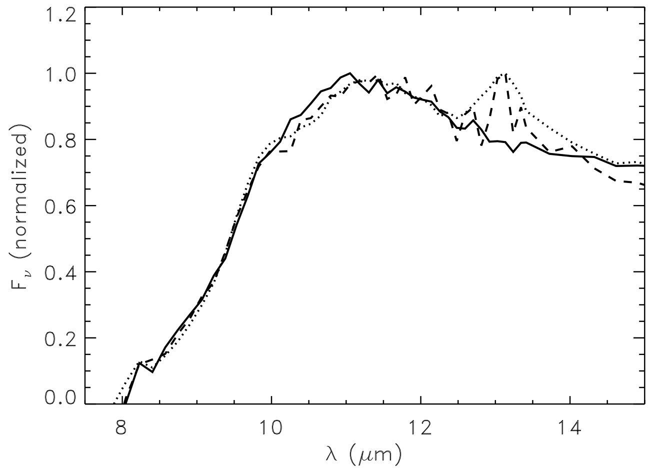

FIG. 9.—Comparison of the dust emission profile for SE3 sources in the AGB sample (*dotted line*), S stars classified with "S class" dust emission by Little-Marenin & Little (1988; *solid line*), and similarly classified oxygen-rich Mira variables (Little-Marenin & Little 1990; *dashed line*).

LML found that 35% of the S stars exhibited S-class dust emission, compared to only 5% of the oxygen-rich Mira variables. These percentages compare favorably to the differences in the distributions with SE class between the AGB sample and the S stars (Fig. 8). Most S stars show SE1–3 dust emission, while the AGB sample is more evenly distributed over the entire SE1–8 range.

4. DISCUSSION

4.1. *The Physical Nature of the Silicate Dust Sequence*

The silicate dust sequence shows that the various dust emission classes identified in the LML system fall along a continuous sequence of dust spectra. A general form for the dust component in equation (1) is

$$S_{\rm dust}(\lambda) = \sum_i B(\lambda, T_i) Q_i(\lambda)(1 - e^{-\tau_i(\lambda)}) , \qquad (6)$$

where the summation is over each component of the dust shell. The total dust spectrum depends on three variables: the temperature of the shell and the optical depth of the shell, both of which depend on the geometry and density of the shell, and the optical efficiencies, which depend primarily on the chemical composition of the dust grains. Thus, the silicate dust sequence must result from the variation in one or more of these properties.

Vardya et al. (1986) and Little-Marenin & Price (1986) suggested a chemical dependence, with the classic emission feature resulting from silicate material and the broad emission feature arising from alumina material (Onaka, de Jong, & Willems 1989). Structured silicate spectra, with emission components at both 10 and 11 μm, resemble spectra seen in comets (Bregman et al. 1987; Hanner, Lynch, & Russell 1994b; Hanner et al. 1994a) and interplanetary dust particles, which are known to contain crystalline silicate grains (Sandford & Walker 1985), and this similarity has led to suggestions that structured silicate emission in circumstellar dust shells arises from crystalline forms of silicates (Tielens 1990; Little-Marenin & Little 1990; Nuth & Hecht 1990).

Ivezic & Elitzur (1995) argue that many of the dust emission classes observed on the silicate dust sequence result only from variations in the optical depth of the shell. To complete the possibilities, Hron, Aringer, & Kerschbaum (1997) suggest that the silicate dust sequence results from variations in the temperature of the dust shell.

The recent set of radiative transfer models by Egan & Sloan (1998) examines these possibilities in detail. They confirm that the upper end of the silicate dust sequence (the classic profile) arises from amorphous silicates, while the lower end of the silicate dust sequence (the broad profile) arises from amorphous alumina materials.

The structured silicate classes present more of a problem. Egan & Sloan (1998) confirm the claim of Ivezic & Elitzur (1995) that increasing the optical depth of a shell of amorphous silicates will drive it down the silicate dust sequence from SE8 to lower indices. It is unlikely, however, that this effect could produce the majority of shells classified below SE5, since as discussed in Paper I, the lower silicate dust sequence shows increasingly blue [12] − [25] colors, while optically thicker models are redder. Nonetheless, the existence of three SB spectra in our AGB sample supports the uncomfortable possibility that at least some fraction of the structured silicate sources are actually unrecognized SB spectra. Until this issue is sorted out, it is impossible to determine what fraction of the structured silicate spectra arise from crystalline silicate grains.

4.2. *The Possible Influence of Photospheric Chemistry*

It is clear that the lower silicate dust sequence (broad emission) results from amorphous alumina grains, while the upper silicate dust sequence (classic emission), results from amorphous silicates. Expressed in these terms, the expansion of the sample in Paper I to include supergiants and S stars reveals that supergiants generally produce dust shells composed of amorphous silicates, while stars with optical spectral classifications of S and MS produce dust shells composed predominantly of amorphous alumina dust. This chemical dichotomy also exists among Mira variables, with symmetric light curves associated with alumina and asymmetric light curves associated with silicates.

The differences in dust chemistry between the supergiants and S stars may provide the key to understanding the origin of the silicate dust sequence. The C/O ratio stays <1 in supergiants owing to the reduced influence of dredge-ups in a more massive envelope (Ritossa, Garciá-Berra, & Iben 1996). For this reason, none of the supergiants are C or S stars. The S stars have higher C/O ratios (~ 1 by definition). We suggest that the differences between the S stars, supergiants, and general AGB sample could arise from how the chemistry of the photosphere manifests itself in the chemistry of the dust grains.

Stencel et al. (1990) argued that the age of a dust shell determines its chemical properties. Alumina grains will condense before silicate grains, owing to the higher condensation temperature of alumina and the greater affinity of oxygen for aluminum compared to silicon. Thus the condensing dust will be alumina-rich initially. Once the aluminum is exhausted, the greater abundances of silicon will lead to dust increasingly dominated by silicates.

We suggest an alternative: it is the C/O abundance of the outflowing gas that drives the chemistry of the dust. In outflows in which the C/O ratio is nearly unity, most of the oxygen will be bound up in CO molecules and will be unavailable for grain condensation. If binding of oxygen and alumina uses up the available oxygen, none will remain to form silicate grains, and alumina grains will dominate the resulting shell. In outflows of progressively lower C/O ratios, the shells will have increasing amounts of silicate grains compared to alumina grains.

Differences in the photospheric chemistry may explain the distribution of SE classes within the general AGB sample as well. High-quality optical spectroscopy of sources on the lower portion of the silicate dust sequence could test this hypothesis by determining what fraction of them are unrecognized S and MS stars. Existing studies have generally avoided dusty stars, owing to the difficulty of obtaining high-quality optical data when a circumstellar shell enshrouds the photosphere.

The dependence of SE index on asymmetry in the light curve of Mira variables leads to the possibility that the shape of the light curve may reflect the C/O ratio in the photosphere. In other words, most stars with symmetric light curves would have to be MS or S stars in which dredge-ups have increased the C/O ratio to values closer to 1. This relationship would explain the even higher values of f seen in carbon-rich Mira variables, where $\langle f \rangle = 48.7 \pm 4.2$ (compare this value to Fig. 5). Again, high-resolution optical spectroscopy could test this hypothesis.

5. CONCLUSION

We have developed a new classification system for infrared dust spectra based on the principles of (1) removing the stellar contribution to the spectrum to isolate the dust emission component and (2) using flux ratios at 10, 11, and 12 μm to quantify the shape of the spectrum. For oxygen-rich dust, this method leads to the silicate dust sequence, along which all previously known spectral classes from oxygen-rich dust can be ordered.

Not only does the silicate dust sequence provide a useful shorthand for describing the dust emission around a star, but it is also a powerful and straightforward diagnostic of the nature of the shell and the star it surrounds. The application of this method to a large sample of optically identified variables on the asymptotic giant branch and on the supergiant branch reveals a number of interesting dependencies with variability type and photospheric C/O ratio. These dependencies provide constraints on the interrelation of the properties of the circumstellar dust shell and the properties of the underlying star, and these constraints may provide the keys to unlocking the continuing mystery of how stars shed their envelopes as they evolve into planetary nebulae or supernovae.

This research made use of the LRS database maintained at the University of Calgary, the SIMBAD database at Strasbourg, and data and software distributed by the NASA

Astronomical Data Center. The authors are grateful for useful discussions with I. R. Little-Marenin, M. P. Egan, P. R. Wood, and C. H. Smith. G. C. S. received support during this project from the Phillips Lab Scholar program, the National Research Council, and NSF grant INT-9703665. G. C. S. also thanks the Physics Department at the University of New England in Armidale, Australia, and the School of Physics, University College, Australian Defence Force Academy, who hosted him during the writing of this paper.

REFERENCES

Bidelman, W. P. 1980, Publ. Warner Swasey Obs., 2(6), 185
Bregman, J. D., Witteborn, F. C., Allamandola, L. J., Campins, H., Wooden, D. H., Rank, D. M., Cohen, M., & Tielens, A. G. G. M. 1987, A&A, 187, 616
Cohen, M., Walker, R. G., & Witteborn, F. C. 1992, AJ, 104, 2030
Cheeseman, P., Stutz, J., Self, M., Taylor, W., Goebel, J., Volk, K., & Walker, H. 1989, Automatic Classification of Spectra from the *Infrared Astronomical Satellite (IRAS)* (NASA RP-1217) (Washington: GPO)
Egan, M. P., & Sloan, G. C. 1998, in preparation
Engelke, C. W. 1992, AJ, 104, 1248
Goebel, J., Volk, K., Walker, H., Gerbault, F., Cheeseman, P., Self, M., Stutz, J., & Taylor, W. 1989, A&A, 222, L5
Hanner, M. S., Hackwell, J. A., Russell, R. W., & Lynch, D. K. 1994a, Icarus, 112, 490
Hanner, M. S., Lynch, D. K., & Russell, R. W. 1994b, ApJ, 425, 274
Hoffmeister, C., Richter, G., & Wenzel, W. 1984, Variable Stars (Berlin: Springer)
Hron, J., Aringer, B., & Kerschbaum, F. 1997, A&A, 322, 280
Ivezic, Z., & Elitzur, M. 1995, ApJ, 445, 415
IRAS Point Source Catalog, Version 2.0. 1988, Joint *IRAS* Science Working Group (Washington: GPO) (PSC)
IRAS Science Team. 1986, A&AS, 65, 607 (LRS Atlas)
Kholopov, P. N., et al. 1985–1988, General Catalogue of Variable Stars (4th ed.; Moscow: Nauka; & Greenbelt: NASA Astronomical Data Center) (GCVS)
Kwok, S., Volk, K., & Bidelman, W. P. 1997, ApJS, 112, 557
Lang, K. R. 1992, Astrophysical Data: Planets & Stars (New York: Springer)
Little-Marenin, I. R., & Little, S. J. 1988, ApJ, 333, 305
———. 1990, AJ, 99, 1173
Little-Marenin, I. R., & Price, S. D. 1986, in Summer School on Interstellar Processes: Abstracts of Contributed Papers, ed. D. J. Hollenbach & H. A. Thronson (NASA Technical Memorandum 88342), 137
Little-Marenin, I. R., Sloan, G. C., & Price, S. D. 1997, in IAU Symp. 177, The Carbon Star Phenomenon, ed. R. F. Wing (Dordrecht: Kluwer), in press
Nuth, J. A., & Hecht, J. H. 1990, Ap&SS, 163, 79
Onaka, T., de Jong, T., & Willems, F. J. 1989, A&A, 218, 169
Ritossa, C., García-Berra, E., & Iben, I. 1996, ApJ, 460, 489
Sandford, S. A., & Walker, R. M. 1985, ApJ, 291, 838
Sloan, G. C., Grasdalen, G. L., & LeVan, P. D. 1993, ApJ, 404, 328
Sloan, G. C., LeVan, P. D., & Little-Marenin, I. R. 1996, ApJ, 463, 310
Sloan, G. C., Little-Marenin, I. R., & Price, S. D. 1998, AJ, 115, 809
Sloan, G. C., & Price, S. D. 1995, ApJ, 451, 758 (Paper I)
Stencel, R. E., Nuth, J. A., Little-Marenin, I. R., & Little, S. J. 1990, ApJ, 350, L45
Tielens, A. G. G. M. 1990, in From Miras to Planetary Nebulae: Which Path for Stellar Evolution?, ed. M. O. Mennessier & A. Omont (Gif-sur-Yvette: Editions Frontières), 186
Vardya, M., de Jong, T., & Willems, F. 1986, ApJ, 304, L29
Volk, K., & Cohen, M. 1989, AJ, 98, 931 (VC)
Walker, R. G., & Cohen, M. 1992, An Atlas of Selected Calibrated Stellar Spectra (NASA Contractor Report 177604)